Genetic Targeting or Pharmacologic Inhibition of NADPH Oxidase Nox4 Provides Renoprotection in Long-Term Diabetic Nephropathy

Genetic Targeting or Pharmacologic Inhibition of NADPH Oxidase Nox4 Provides Renoprotection in Long-Term Diabetic Nephropathy

Jay C. Jha,*† Stephen P. Gray,* David Barit,* Jun Okabe,‡ Assam El-Osta,‡ Tamehachi Namikoshi,*§ Vicki Thallas-Bonke,* Kirstin Wingler,‖ Cedric Szyndralewiez,¶ Freddy Heitz,¶ Rhian M. Touyz,**†† Mark E. Cooper,*† Harald H.H.W. Schmidt,‖ and Karin A. Jandeleit-Dahm*†

*Diabetic Complications Division, Juvenile Diabetes Research Foundation Danielle Alberti Memorial Centre for Diabetic Complications, Baker IDI Heart & Diabetes Institute, Melbourne, Victoria, Australia; †Department of Medicine, Monash University, Melbourne, Victoria, Australia; ‡Human Epigenetics Laboratory, Baker IDI Heart & Diabetes Institute, Melbourne, Victoria, Australia; §Department of Nephrology and Hypertension, Kawasaki Medical School, Kurashiki, Japan; ‖Department of Pharmacology, Cardiovascular Research Institute Maastricht, Faculty of Medicine, Health & Life Science, Maastricht University, Maastricht, The Netherlands; ¶Genkyotex SA, Geneva, Switzerland; **Ottawa Hospital Research Institute, Ottawa, Ontario, Canada; and ††Institute of Cardiovascular and Medical Sciences, University of Glasgow, Glasgow, United Kingdom

ABSTRACT

Diabetic nephropathy may occur, in part, as a result of intrarenal oxidative stress. NADPH oxidases comprise the only known dedicated reactive oxygen species (ROS)–forming enzyme family. In the rodent kidney, three isoforms of the catalytic subunit of NADPH oxidase are expressed (Nox1, Nox2, and Nox4). Here we show that Nox4 is the main source of renal ROS in a mouse model of diabetic nephropathy induced by streptozotocin administration in *ApoE*$^{-/-}$ mice. Deletion of Nox4, but not of Nox1, resulted in renal protection from glomerular injury as evidenced by attenuated albuminuria, preserved structure, reduced glomerular accumulation of extracellular matrix proteins, attenuated glomerular macrophage infiltration, and reduced renal expression of monocyte chemoattractant protein-1 and NF-κB in streptozotocin-induced diabetic *ApoE*$^{-/-}$ mice. Importantly, administration of the most specific Nox1/4 inhibitor, GKT137831, replicated these renoprotective effects of Nox4 deletion. In human podocytes, silencing of the Nox4 gene resulted in reduced production of ROS and downregulation of proinflammatory and profibrotic markers that are implicated in diabetic nephropathy. Collectively, these results identify Nox4 as a key source of ROS responsible for kidney injury in diabetes and provide proof of principle for an innovative small molecule approach to treat and/or prevent chronic kidney failure.

J Am Soc Nephrol 25: 1237–1254, 2014. doi: 10.1681/ASN.2013070810

CKD is a major complication of diabetes. Furthermore, diabetes remains the most common cause of end stage renal failure and need for kidney transplantation.[1] The underlying mechanisms responsible for diabetic nephropathy remain to be fully defined. Therefore, effective and mechanism-based therapies are not available. It has been hypothesized that diabetes mellitus causes renal oxidative stress, that is, increased levels of reactive oxygen species (ROS), resulting in glomerular damage. Accordingly, oxidative stress is increasingly considered to be a major

Received July 30, 2013. Accepted November 5, 2013.

H.H.H.W.S. and K.A.J.-D. contributed equally to this work.

Published online ahead of print. Publication date available at www.jasn.org.

Correspondence: Dr. Karin Jandeleit-Dahm, Diabetes Complications Division, Baker IDI Heart & Diabetes Research Institute, PO Box 6492 St Kilda Road, Melbourne, Victoria 8008, Australia. Email: karin.jandeleit-dahm@bakeridi.edu.au

contributor to the development and progression of diabetic nephropathy.[2] Various renal sources of ROS have been suggested to be relevant in the diabetic kidney. These include auto-oxidation of glucose, advanced glycation, glycolysis, glucose-6-phosphate dehydrogenase, sorbitol/polyol pathway flux, hexosamine pathway flux, mitochondrial respiratory chain, xanthine oxidase, uncoupled nitric oxide synthase, and NADPH oxidases.[2,3]

Among these sources, NADPH oxidases are suggested to play a pivotal role in the development and progression of renal injury in animal models of type 1 and type 2 diabetic nephropathy[4–6] and hence represent a potentially important novel target. NADPH oxidases are the only enzymes known to be solely dedicated to ROS generation. Seven isoforms of their catalytic subunit exist (Nox1–5; Duox1 and 2). Nox isoforms depend to varying degrees on additional subunits.[7–10] Among these isoforms, Nox1, Nox2, and Nox4 are expressed in the renal cortex. In streptozotocin-induced diabetic nephropathy, expression of Nox4, Nox2, and another subunit, p22phox, are all upregulated.[11–13] With respect to Nox2, our own studies in streptozotocin-induced diabetic Nox2 knockout (KO) mice have shown increased susceptibility to infections and 100% mortality at week 20 of diabetes.[14] We thus did not consider Nox2 blockade a priority in this study addressing strategies to reduce diabetic nephropathy.

Nox4, originally termed Renox, is highly expressed in renal tissues.[15–18] The role of Nox4 in diabetic nephropathy remains controversial. Nox4 downregulation by systemic administration of antisense oligonucleotides, albeit for a short period of only 2 weeks, reduced renal and glomerular hypertrophy and attenuated the increased expression of fibronectin in renal cortex and glomeruli in streptozotocin-induced diabetic rats.[19] However, the Nox4 antisense oligonucleotide may not be absolutely specific for Nox4. Furthermore, other authors have suggested either no effect[20] or a protective role of Nox4 in diabetic nephropathy or in other models of renal fibrosis.[21] With respect to Nox1, this isoform appears to play a major role in diabetic macrovascular disease[14]but not much is known about the role of Nox1 in diabetic nephropathy. Thus, it remains to be determined which Nox isoform plays the most critical role in diabetic kidney disease.

Here we report for the first time a direct comparison of the long-term effects of Nox1 and Nox4 deletion in the development and progression of diabetic nephropathy, by directly comparing renal injury in streptozotocin-induced diabetic $Nox1^{-/y}ApoE^{-/-}$ and $Nox4^{-/-}ApoE^{-/-}$ double KO mice and their respective wild-type (WT) control mice. In addition, the genetic deletion studies were complemented by a pharmacologic intervention study using the currently most specific Nox inhibitor, GKT137831.[22] Key findings in the *in vivo* studies were confirmed *in vitro* using human podocytes.

RESULTS

Metabolic Parameters

First, we investigated the effects of Nox1 and Nox4 deletion as well as GKT137831 treatment on metabolic control in diabetic mice. Induction of diabetes was associated with reduced body weight, elevated plasma glucose, and glycated hemoglobin levels in diabetic $Nox4^{+/+}ApoE^{-/-}$, $Nox1^{+/y}ApoE^{-/-}$, and $ApoE^{-/-}$ mice compared with their respective nondiabetic controls. Diabetic animals also showed a significant elevation in serum cholesterol, triglyceride, and LDL levels compared with their respective nondiabetic controls. Neither genetic deletion of Nox4 or Nox1 had any effect on the diabetes-induced changes in body weight, glycemic control, or lipid parameters (Table 1). Furthermore, no changes in metabolic parameters were seen with pharmacologic Nox inhibition using GKT137831 in $ApoE^{-/-}$ mice for 20 weeks (Table 2). In addition, systolic BP was similar in all groups. The kidney weight/body weight ratio was significantly increased in diabetic mice. This tended to be attenuated in diabetic $Nox4^{-/-}ApoE^{-/-}$ mice compared with diabetic $Nox4^{+/+}ApoE^{-/-}$ mice ($P=0.08$) and was significantly reduced in GKT137831-treated diabetic $ApoE^{-/-}$ mice compared with untreated diabetic $ApoE^{-/-}$ mice ($P<0.05$). However, the kidney weight/body weight ratio was unchanged in diabetic $Nox1^{-/y}ApoE^{-/-}$ mice compared with diabetic $Nox1^{+/y}ApoE^{-/-}$ mice (Tables 1 and 2).

Renal Function Parameters

Albuminuria is a key feature of diabetic nephropathy. Therefore, we investigated the effect of Nox1 or Nox4 deletion on albuminuria development and compared the effects to treatment with the Nox inhibitor, GKT137831, in diabetic $ApoE^{-/-}$ mice. Albuminuria tended to be reduced after 10 weeks of diabetes in $Nox4^{-/-}ApoE^{-/-}$ mice compared with diabetic $Nox4^{+/+}ApoE^{-/-}$ mice, but this effect did not reach statistical significance (Figure 1A). However, after 20 weeks of diabetes, albuminuria was significantly attenuated in diabetic $Nox4^{-/-}ApoE^{-/-}$ mice compared with diabetic $Nox4^{+/+}ApoE^{-/-}$ mice ($P<0.05$) (Figure 1A). Similarly to deleting Nox4, GKT137831 treatment of diabetic $ApoE^{-/-}$ mice protected against development of albuminuria after 10 and 20 weeks of diabetes (Figure 1C). In contrast, albuminuria was unaffected in diabetic $Nox1^{-/y}ApoE^{-/-}$ mice (Figure 1B). Similar effects were also observed when the data were expressed as the urinary albumin/creatinine ratio after 10 and 20 weeks of diabetes (Figure 1, D–F).

Renal Structural Assessment

Diabetic nephropathy is associated with structural abnormalities including glomerulosclerosis and specifically mesangial expansion. Indeed, glomerulosclerosis and mesangial area expansion were significantly increased after 20 weeks of diabetes in $Nox4^{+/+}ApoE^{-/-}$ mice compared with nondiabetic $Nox4^{+/+}ApoE^{-/-}$ mice. In diabetic $Nox4^{-/-}ApoE^{-/-}$ mice, the development of glomerulosclerosis and the degree of mesangial expansion were significantly attenuated compared with diabetic $Nox4^{+/+}ApoE^{-/-}$ mice after 20 weeks of diabetes (Figure 2, A and B). These renoprotective structural changes were not observed in diabetic $Nox1^{-/y}ApoE^{-/-}$ mice compared with diabetic $Nox1^{+/y}ApoE^{-/-}$ mice (Figure 2, C and D).

Table 1. General and metabolic parameters after 20 weeks of study in control and diabetic *Nox4*$^{+/+}$*ApoE*$^{-/-}$ and *Nox4*$^{-/-}$*ApoE*$^{-/-}$ mice and in control and diabetic *Nox1*$^{+/y}$*ApoE*$^{-/-}$ and *Nox1*$^{-/y}$ *ApoE*$^{-/-}$ mice (*n*=8–15 per group)

Parameter	Nox4 Deletion				Nox1 Deletion			
	Nox4$^{+/+}$*ApoE*$^{-/-}$		*Nox4*$^{-/-}$*ApoE*$^{-/-}$		*Nox1*$^{+/y}$*ApoE*$^{-/-}$		*Nox1*$^{-/y}$*ApoE*$^{-/-}$	
	Control	Diabetes	Control	Diabetes	Control	Diabetes	Control	Diabetes
Body weight (g)	33±0.6	22±0.9[a]	31±0.6	25±0.8[a]	32±1	23±1[a]	34±1	25±1[a]
Kidney weight/body weight (%)	0.61±0.01	0.94±0.05[a]	0.61±0.02	0.82±0.01[a]	0.62±0.02	0.87±0.05[a]	0.58±0.01	0.90±0.02[a]
Systolic BP (mmHg)	91±2.7	110±7.0	93±5.4	99±4.7	104±4	106±4	100±3	101±2
Plasma glucose (mmol/L)	10.4±0.6	25.0±2.2[a]	11.2±0.6	24.3±1.3[a]	13.1±0.9	26.2±2.3[a]	12.7±0.4	29.6±1.4[a]
Glycated hemoglobin (%)	4.9±0.3	15.4±0.9[a]	7.8±0.9[b]	18.9±1.2[a]	4.8±0.4	18 0.9±1.5[a]	4.6±0.3	18.7±1.8[a]
Total cholesterol (mmol/L)	5.8±1.2	13.7±1.8[a]	8.2±0.4	16.3±1.8[a]	7.6±0.6	10.3±1.0[a]	7.3±0.6	14.4±1.7[a,c]
Triglycerides (mmol/L)	1.2±0.2	3.4±0.5[a]	0.8±0.1	5.0±0.9[a]	1.0±0.1	2.3±0.5[a]	1.2±0.2	3.7±0.6[a]
HDL (mmol/L)	1.2±0.3	2.5±0.5[a]	1.9±0.1	2.3±0.4	1.7±0.2	1.5±0.2	1.7±0.2	2.8±0.3[a,c]
LDL (mmol/L)	4.0±0.8	9.7±1.2[a]	5.9±0.3	11.7±1.2[a]	5.4±0.5	6.9±1.0[a]	5.0±0.4	10.0±1.2[a]

Data are the mean±SEM.
[a]$P<0.05$ versus respective control *Nox4*$^{+/+}$*ApoE*$^{-/-}$ or *Nox4*$^{-/-}$*ApoE*$^{-/-}$ or control *Nox1*$^{+/y}$*ApoE*$^{-/-}$ and *Nox1*$^{-/y}$*ApoE*$^{-/-}$ mice.
[b]$P<0.05$ versus control *Nox4*$^{+/+}$*ApoE*$^{-/-}$ mice.
[c]$P<0.05$ versus diabetic *Nox1*$^{+/y}$*ApoE*$^{-/-}$ mice.

Table 2. General and metabolic parameters after 20 weeks of study in control and diabetic *ApoE*$^{-/-}$ mice, with and without treatment with GKT137831 (*n*=8–15 per group)

Parameter	Nox Inhibition			
	ApoE$^{-/-}$		*ApoE*$^{-/-}$+GKT137831	
	Control	Diabetes	Control	Diabetes
Body weight (g)	31±0.5	25±0.7[a]	28±0.6	24±0.9[a]
Kidney weight/body weight (%)	0.60±0.01	0.95±0.05[a]	0.58±0.01	0.77±0.03[a,b]
Systolic BP (mmHg)	105±3.0	113±4.7	107±3.4	98±6.3
Plasma glucose (mmol/L)	11.8±0.4	24.8±1.0[a]	13.6±0.5	28.9±1.5[a]
Glycated hemoglobin (%)	5.0±0.3	17.4±0.9[a]	5±0.07	15.7±1.6[a]
Total cholesterol (mmol/L)	6.7±0.5	13.3±1.9[a]	7.6±0.8	11.4±1.2[a]
Triglycerides (mmol/L)	1.2±0.1	3.2±0.7[a]	1.2±0.3	2.3±0.5[a]
HDL (mmol/L)	1.6±0.2	2.0±0.3	1.7±0.3	1.9±0.2
LDL (mmol/L)	4.6±0.3	9.8±1.4[a]	5.4±0.5	8.4±0.9[a]

Data are the mean±SEM.
[a]$P<0.05$ versus respective control *ApoE*$^{-/-}$ and *ApoE*$^{-/-}$ plus GKT137831.
[b]$P<0.05$ versus diabetic *ApoE*$^{-/-}$ mice.

Treatment of diabetic *ApoE*$^{-/-}$ mice with the Nox inhibitor GKT137831 for 20 weeks was also associated with attenuation of glomerular injury, as assessed by the glomerulosclerosis index (Figure 2E) and mesangial area (Figure 2F). These results suggest that genetic deletion of Nox4 and Nox inhibition with GKT137831 in diabetic *ApoE*$^{-/-}$ mice confer renoprotective effects with respect to structural parameters. No such effect was seen with deletion of Nox1. Furthermore, there was an increase in the tubulointerstitial area in diabetic *ApoE*$^{-/-}$ mice (Supplemental Figure 1). Indeed, the Nox inhibitor, GKT137831, significantly attenuated the tubulointerstitial area (Supplemental Figure 1, C and D). There was a similar trend seen in diabetic *Nox4*$^{-/-}$*ApoE*$^{-/-}$ mice (P=0.07) (Supplemental Figure 1, A and B).

Nox4 Expression

Induction of diabetes was associated with increased gene expression of Nox4 as well as Nox1 and Nox2 in renal cortex (Supplemental Figure 2A). In addition, Nox4 gene expression was also increased in the tubular fraction of the renal cortex of diabetic mice (Supplemental Figure 2C). Furthermore, there was an increase in both glomerular and tubular Nox4 protein expression, as assessed by immunofluorescence (Supplemental Figure 2, B and D). By contrast, there was no significant Nox4 expression in the Nox4 KO mice in the absence or presence of diabetes.

Extracellular Matrix Proteins

We next examined glomerular collagen IV and fibronectin accumulation, which are known to be associated with glomerulosclerosis and mesangial expansion in diabetic nephropathy. Consistent with the findings on glomerulosclerosis and mesangial expansion, collagen IV protein accumulation was significantly increased in the glomeruli after 20 weeks of diabetes in *Nox4*$^{+/+}$*ApoE*$^{-/-}$ mice compared with nondiabetic *Nox4*$^{+/+}$*ApoE*$^{-/-}$ controls. Importantly, the increase in collagen IV expression was attenuated in *Nox4*$^{-/-}$*ApoE*$^{-/-}$ mice (Figure 3A). In contrast, this reduction in collagen IV expression was not observed in *Nox1*$^{-/y}$*ApoE*$^{-/-}$ mice compared with diabetic *Nox1*$^{+/y}$*ApoE*$^{-/-}$ mice (Figure 3B). Furthermore, Nox inhibition with GKT137831 in diabetic *ApoE*$^{-/-}$ mice for 20 weeks was associated with a significant attenuation of the diabetes-induced increased expression of collagen IV (Figure 3C). Similarly, fibronectin protein accumulation was increased in the glomeruli of mice after 20

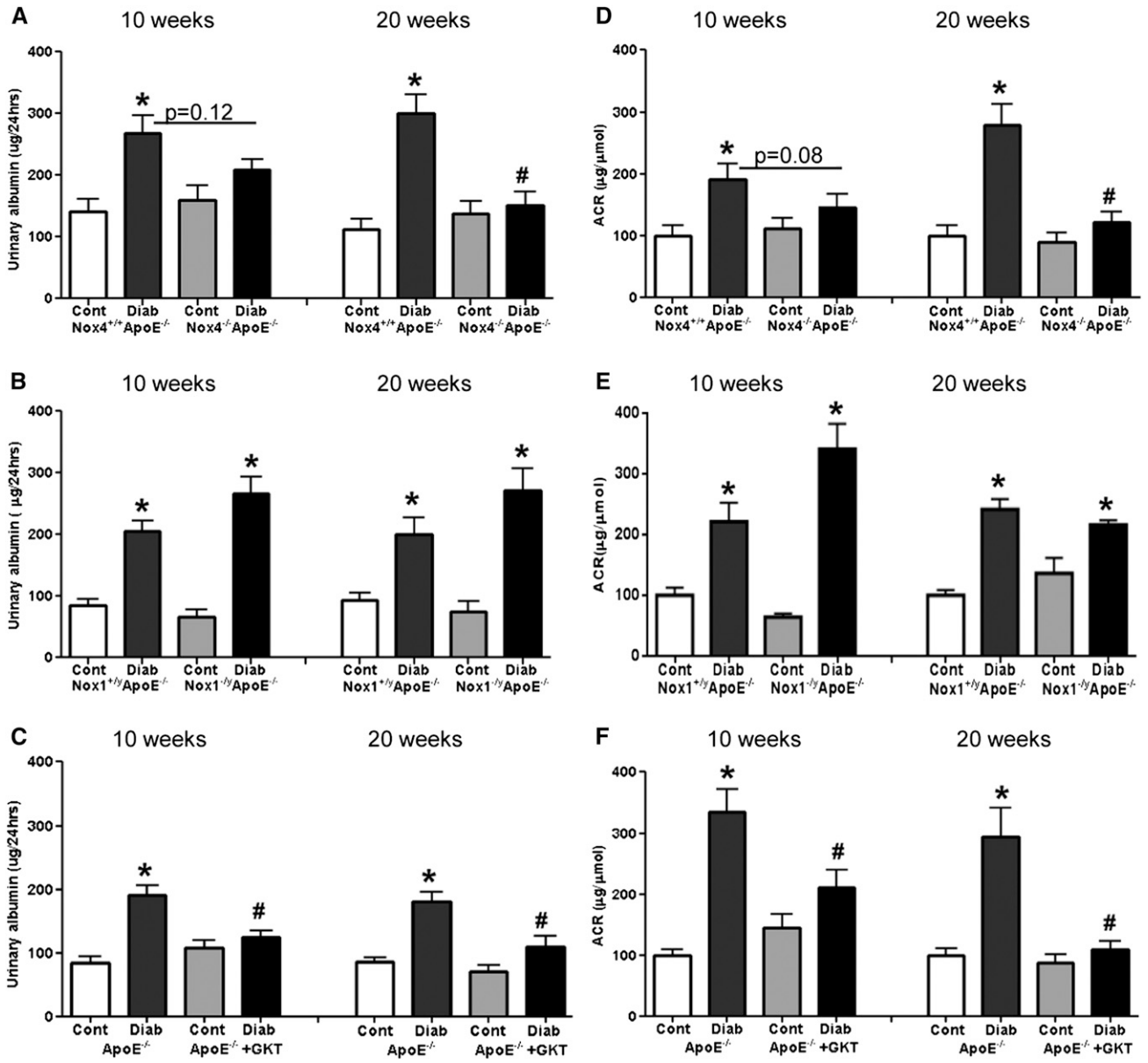

Figure 1. Genetic deficiency of Nox4, but not of Nox1, and pharmacologic Nox inhibition attenuate diabetes-induced increased albuminuria in diabetic $ApoE^{-/-}$ mice. Urinary albumin excretion (A–C) and ACR (D–F) in control and diabetic $Nox4^{+/+}ApoE^{-/-}$ and $Nox4^{-/-}ApoE^{-/-}$ mice (A and D), control and diabetic $Nox1^{+/y}ApoE^{-/-}$ and $Nox1^{-/y}ApoE^{-/-}$ mice (B and E), or control and diabetic $ApoE^{-/-}$ mice with and without treatment with GKT137831 (C and F) for 10 and 20 weeks (n=10–15 per group). Data are the mean±SEM. *P<0.01 versus respective control $Nox4^{+/+}ApoE^{-/-}$ and $Nox4^{-/-}ApoE^{-/-}$ mice (A and D), control $Nox1^{+/y}ApoE^{-/-}$ and $Nox1^{-/y}ApoE^{-/-}$ mice (B and E), or control $ApoE^{-/-}$ and $ApoE^{-/-}$ plus GKT137831 mice (C and F); #P<0.05 versus diabetic $Nox4^{+/+}ApoE^{-/-}$ (A and D) or diabetic $ApoE^{-/-}$ mice (C and F). ACR, albumin/creatinine ratio; Cont, control; Diab, diabetes; GKT, GKT137831.

weeks of diabetes, and this was prevented in mice with deletion of Nox4 (Figure 4A) but not with deletion of Nox1 (Figure 4B). Again, GKT137831 treatment of diabetic $ApoE^{-/-}$ mice for 20 weeks resulted in attenuated diabetes-induced increased expression of fibronectin (Figure 4C).

We previously showed that renal vascular endothelial growth factor (VEGF) expression is increased in experimental diabetes and is associated with albuminuria.[23] Indeed, we observed that VEGF expression was higher in the glomeruli of diabetic $Nox4^{+/+}ApoE^{-/-}$ mice compared with nondiabetic controls, and this was attenuated in diabetic $Nox4^{-/-}ApoE^{-/-}$ mice (Figure 5A). Furthermore, GKT137831 treatment of diabetic $ApoE^{-/-}$ mice for 20 weeks was also associated with decreased expression of VEGF in the glomeruli of diabetic $ApoE^{-/-}$ mice (Figure 5B).

Together, these results suggest that genetic deletion of Nox4, but not of Nox1, protects mice from renal functional and structural changes associated with diabetic nephropathy *via*

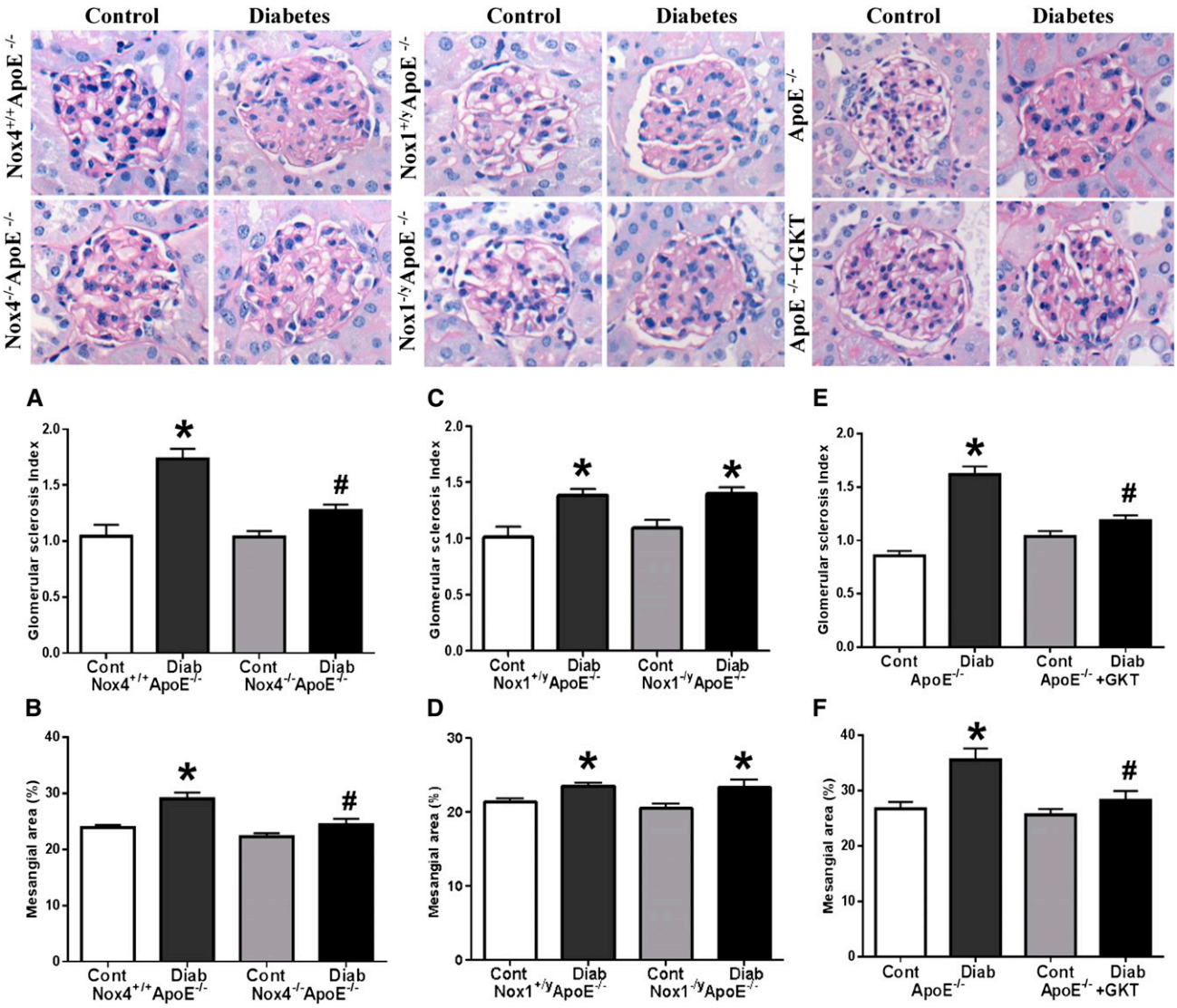

Figure 2. Genetic deficiency of Nox4, but not of Nox1, and pharmacologic Nox inhibition attenuate glomerular injury in diabetic $ApoE^{-/-}$ mice. Glomerulosclerosis index (A) and mesangial area expansion (B) in control and diabetic $Nox4^{+/+}ApoE^{-/-}$ and $Nox4^{-/-}ApoE^{-/-}$ mice after 20 weeks (n=7–8 per group). Glomerulosclerosis index (C) and mesangial area expansion (D) in control and diabetic $Nox1^{+/y}ApoE^{-/-}$ and $Nox1^{-/y}ApoE^{-/-}$ mice after 20 weeks (n=7–8 per group). Glomerulosclerosis index (E) and mesangial area expansion (F) in control and diabetic $ApoE^{-/-}$ mice with and without treatment with GKT137831 for 20 weeks (n=7–8 per group). Data are the mean±SEM. *P<0.01 versus respective control $Nox4^{+/+}ApoE^{-/-}$ and $Nox4^{-/-}ApoE^{-/-}$ mice (A and B), control $Nox1^{+/y}ApoE^{-/-}$ and $Nox1^{-/y}ApoE^{-/-}$ mice (C and D), or control $ApoE^{-/-}$ and $ApoE^{-/-}$ plus GKT137831 mice (E and F); #P<0.05 versus diabetic $Nox4^{+/+}ApoE^{-/-}$ (A and B) or diabetic $ApoE^{-/-}$ mice (E and F). Cont, control; Diab, diabetes; GKT, GKT137831.

effects on glomerulosclerosis, mesangial expansion, collagen IV, and fibronectin accumulation. Treatment of diabetic $ApoE^{-/-}$ mice with the specific Nox inhibitor GKT137831 for 20 weeks resulted in similar renoprotection as observed in Nox4-deficient $ApoE^{-/-}$ mice, which provides a proof of concept for Nox inhibition as a novel therapeutic strategy for diabetic nephropathy.

Renal Superoxide and ROS Levels

There is increasing evidence that renal injury in diabetes is associated with increased formation of ROS.[2,4–6] Indeed, nitrotyrosine, a marker of nitrative and oxidative stress, was increased in glomeruli after 20 weeks of diabetes in $Nox4^{+/+}ApoE^{-/-}$ and $ApoE^{-/-}$ mice. Importantly, diabetic $Nox4^{-/-}ApoE^{-/-}$ mice and GKT137831-treated diabetic $ApoE^{-/-}$ mice showed reduced nitrotyrosine accumulation in the glomeruli compared with diabetic $Nox4^{+/+}ApoE^{-/-}$ and non-treated diabetic $ApoE^{-/-}$ mice, respectively (Figure 6, A and C). In line with our above-described observations, no reduction of nitrotyrosine was observed in diabetic $Nox1^{-/y}ApoE^{-/-}$ mice compared with diabetic $Nox1^{+/y}ApoE^{-/-}$ mice (Figure 6B).

We also measured superoxide generation in the renal cortex using the dihydroethidium/HPLC method (Figure 7, A, C, and

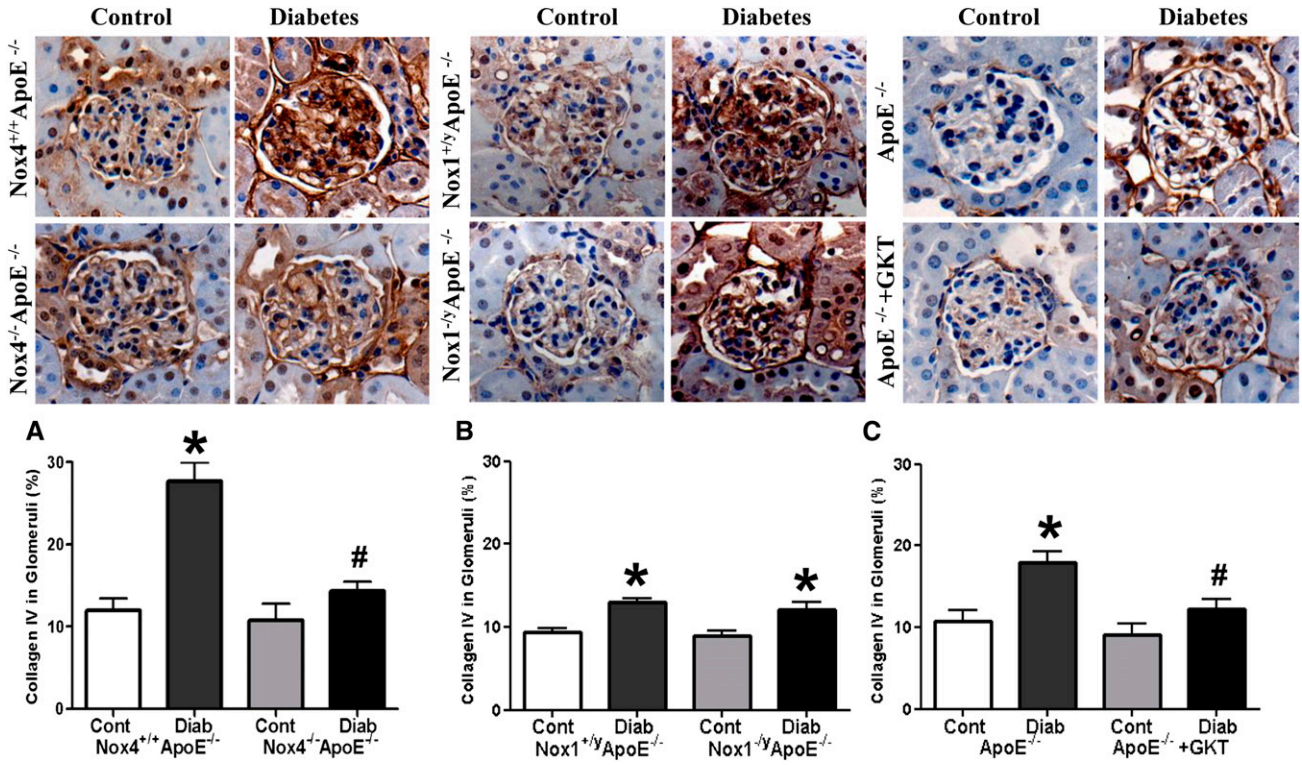

Figure 3. Genetic deficiency of Nox4, but not of Nox1, and pharmacologic Nox inhibition attenuate increased collagen IV accumulation in glomeruli of diabetic $ApoE^{-/-}$ mice. Immunostaining for collagen IV in glomeruli of control and diabetic $Nox4^{+/+}ApoE^{-/-}$ and $Nox4^{-/-}ApoE^{-/-}$ mice after 20 weeks (A), control and diabetic $Nox1^{+/y}ApoE^{-/-}$ and $Nox1^{-/y}ApoE^{-/-}$ mice after 20 weeks (B), or control and diabetic $ApoE^{-/-}$ mice with and without treatment with GKT137831 for 20 weeks (C) (n=6–8 per group). Data are the mean±SEM. *P<0.05 versus respective control $Nox4^{+/+}ApoE^{-/-}$ and $Nox4^{-/-}ApoE^{-/-}$ mice (A), control $Nox1^{+/y}ApoE^{-/-}$ and $Nox1^{-/y}ApoE^{-/-}$ mice (B), or control $ApoE^{-/-}$ and $ApoE^{-/-}$ plus GKT137831 mice (C); #P<0.05 versus diabetic $Nox4^{+/+}ApoE^{-/-}$ (A) or diabetic $ApoE^{-/-}$ mice (C). Cont, control; Diab, diabetes; GKT, GKT137831.

E)[14,24] as well as ROS levels in the cytosolic and mitochondrial fractions of the renal cortex using L-012–derived chemiluminescence (Figure 7, B, D, and F). Diabetes was associated with increased renal superoxide levels in the renal cortex (Figure 7, A, C, and E). In addition, diabetes was associated with increased ROS levels in both the cytosolic and mitochondrial compartments (Figure 7, B, D, and F). Diabetic $ApoE^{-/-}$ mice with genetic Nox4 deficiency did not show the diabetes-induced increase in superoxide (Figure 7A) or ROS formation in either intracellular compartment (Figure 7B). Similar results were obtained in diabetic $ApoE^{-/-}$ mice treated with GKT137831 for 20 weeks (Figure 7, E and F). Again, this effect on reducing superoxide and ROS levels was not seen in Nox1-deficient diabetic mice ($Nox1^{-/y}ApoE^{-/-}$ mice) (Figure 7, C and D). These results suggest that renoprotection observed with Nox4 deletion and pharmacologic Nox inhibition is associated with reduced renal ROS formation. The results further support the view that Nox4, but not Nox1, is a pathologically relevant source of ROS in diabetic nephropathy.

Macrophage Infiltration

Diabetes is associated with recruitment and retention of macrophages in glomeruli.[25] Accordingly, expression of the macrophage marker F4/80 in glomeruli of diabetic mice after 20 weeks of diabetes was increased in diabetic $Nox4^{+/+}ApoE^{-/-}$ and $ApoE^{-/-}$ mice compared with their nondiabetic controls. Again, this parameter was attenuated in diabetic $Nox4^{-/-}ApoE^{-/-}$ mice (Figure 8A) and in diabetic $ApoE^{-/-}$ mice treated with GKT137831 (Figure 8C). In contrast, expression of F4/80 in glomeruli of diabetic $Nox1^{-/y}ApoE^{-/-}$ mice was not different from diabetic $Nox1^{+/y}ApoE^{-/-}$ mice (Figure 8B).

Human Podocyte *In Vitro* Studies

Podocytes are considered to be centrally involved in regulation of the glomerular filtration barrier and development of proteinuria.[26] We therefore investigated the effects of hyperglycemia and TGF-β1, which are both key features of the diabetic milieu, on ROS formation and markers of diabetes-related injury in a human differentiated podocyte cell line as previously described (Supplemental Figure 3).[27] Under nonpermissive conditions, the podocytes undergo growth arrest, display the typical arborized pattern of foot process extensions, and express markers of mature podocytic differentiation including nephrin, synaptopodin, and Wilms' tumor-1 (Supplemental Figure 4).

Incubation of human podocytes in high glucose–containing medium (25 mM, *i.e.*, similar glucose concentrations to those

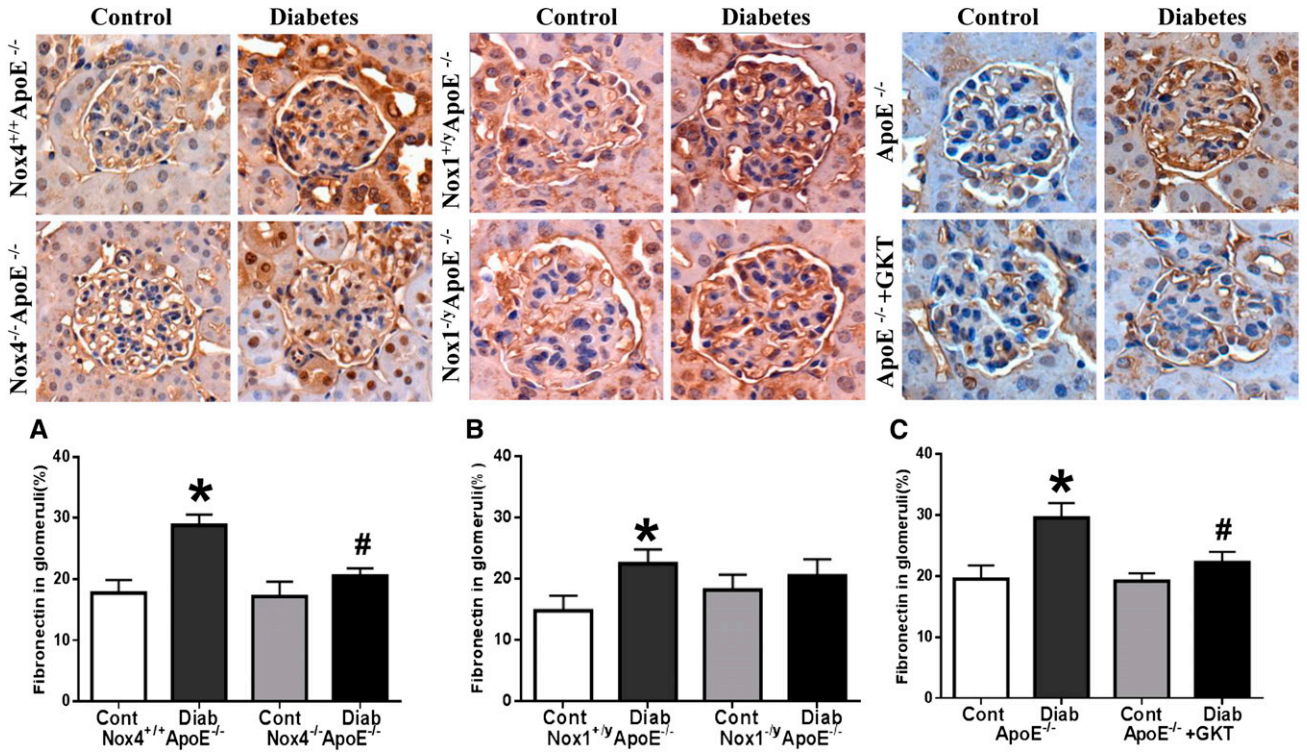

Figure 4. Genetic deficiency of Nox4, but not of Nox1, and pharmacologic Nox inhibition attenuate increased fibronectin accumulation in glomeruli of diabetic *ApoE*$^{-/-}$ mice. Immunostaining for fibronectin in glomeruli of control and diabetic *Nox4*$^{+/+}$*ApoE*$^{-/-}$ and *Nox4*$^{-/-}$*ApoE*$^{-/-}$ mice after 20 weeks (A), control and diabetic *Nox1*$^{+/y}$*ApoE*$^{-/-}$ and *Nox1*$^{-/y}$*ApoE*$^{-/-}$ mice after 20 weeks (B), or control and diabetic *ApoE*$^{-/-}$ mice with and without treatment with GKT137831 for 20 weeks (C) (n=6–8 per group). Data are the mean±SEM. *P<0.05 versus respective control *Nox4*$^{+/+}$*ApoE*$^{-/-}$ and *Nox4*$^{-/-}$*ApoE*$^{-/-}$ mice (A), control *Nox1*$^{+/y}$*ApoE*$^{-/-}$ and *Nox1*$^{-/y}$ *ApoE*$^{-/-}$ mice (B), or control *ApoE*$^{-/-}$ and *ApoE*$^{-/-}$ plus GKT137831 mice (C); $^{\#}P$<0.05 versus diabetic *Nox4*$^{+/+}$*ApoE*$^{-/-}$ (A) or diabetic *ApoE*$^{-/-}$ mice (C). Cont, control; Diab, diabetes; GKT, GKT137831.

observed in the serum of our streptozotocin-treated mice) resulted in increased mRNA levels of Nox4 (Figure 9A). The addition of TGF-β to this hyperglycemic milieu further amplified the increase in Nox4 gene expression and to a lesser extent also increased Nox5, but not Nox1, Nox2, or their cytosolic regulator, p47phox. The iso-osmotic control mannitol did not result in changes in any Nox isoform levels (Figure 9A). Furthermore, Nox4 protein was expressed in these podocytes, as assessed by immunofluorescence (Supplemental Figure 5).

We next infected human podocytes with a lentiviral Nox4 short hairpin RNA (shRNA) expression construct. This resulted in a decrease in Nox4 gene expression of approximately 70% (Supplemental Figure 6). Nox4 shRNA treatment of the podocytes did not change the mRNA levels of Nox1, Nox2, or Nox5 (Supplemental Figure 6). Importantly, the high glucose– and TGF-β1–induced increase in ROS production was reduced in Nox4 knockdown cells to ROS levels seen in podocytes in normal glucose or in cells that had not been treated with TGF-β1 (Figure 9, B and D).

High glucose alone increased the gene expression of the extracellular matrix (ECM) proteins, collagen IV, and fibronectin as well as VEGF, whereas the effect on α-smooth muscle actin (α-SMA) did not reach statistical significance (Figure 9C). The addition of TGF-β significantly increased gene expression of collagen IV, fibronectin, VEGF, and α-SMA (Figure 9E). Silencing of Nox4 by infecting the podocytes with a Nox4 shRNA led to a decrease in both the glucose– and TGF-β–induced increased expression of collagen IV, fibronectin, VEGF, and α-SMA compared with cells infected with nontargeted control constructs (Figure 9, C and E).

TGF-β– and high glucose–induced upregulation of Nox4 with an associated increase in ROS formation was attenuated by pretreatment of human podocytes with the Nox inhibitor GKT137831 (Figure 10A). Furthermore, the increased expression of collagen IV, fibronectin, connective tissue growth factor, VEGF, and α-SMA as a result of high glucose and TGF-β were significantly attenuated when cells were pretreated with GKT137831 (Figure 10B).

Inflammatory Parameters: Monocyte Chemoattractant Protein-1 and NF-κB

We further investigated the effect of Nox4 deletion on the NF-κB/monocyte chemoattractant protein-1 (MCP-1) axis, a pathway that has been implicated in the development of diabetic nephropathy.[25] Consistent with the results observed with respect to macrophage infiltration into the kidney (Figure

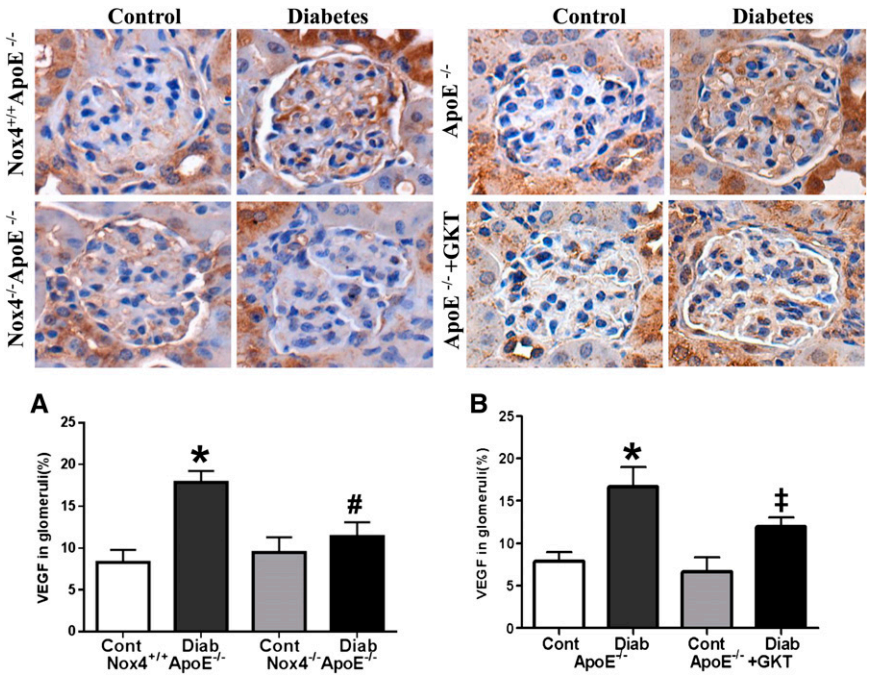

Figure 5. Genetic deficiency of Nox4 and pharmacologic Nox inhibition attenuate increased VEGF expression in glomeruli of diabetic $ApoE^{-/-}$ mice. Immunostaining for VEGF in glomeruli of control and diabetic $Nox4^{+/+}ApoE^{-/-}$ and $Nox4^{-/-}ApoE^{-/-}$ mice after 20 weeks (A) and control and diabetic $ApoE^{-/-}$ mice with and without treatment with GKT137831 for 20 weeks (B) (n=6–8 per group). Data are the mean±SEM. *P<0.05 versus respective control $Nox4^{+/+}ApoE^{-/-}$ and $Nox4^{-/-}ApoE^{-/-}$ mice (A) or control $ApoE^{-/-}$ and $ApoE^{-/-}$ plus GKT137831 mice (B); #P<0.05 versus diabetic $Nox4^{+/+}ApoE^{-/-}$ (A); ‡P=0.08 versus diabetic $ApoE^{-/-}$ mice (B). Cont, control; Diab, diabetes; GKT, GKT137831.

8), we observed upregulation of the MCP-1 gene in the renal cortex of diabetic mice, which was significantly attenuated in the diabetic Nox4-deficient mice (Figure 11C). There was also a trend toward a decrease in the diabetes-induced upregulation of the NF-κB subunit p65 in the renal cortex of Nox4 KO mice (Figure 11D). To complement these *in vivo* findings, *in vitro* studies were performed in human podocytes. Indeed, silencing of Nox4 abrogated the high glucose–induced upregulation of MCP-1 and p65 mRNA levels (Figure 11, A and B).

In addition, expression of MCP-1 in protein extracts of renal cortex after 20 weeks of diabetes was increased in diabetic $Nox4^{+/+}ApoE^{-/-}$ and $ApoE^{-/-}$ mice compared with their nondiabetic controls. Again, this parameter was attenuated in diabetic $Nox4^{-/-}ApoE^{-/-}$ mice (Figure 11E) and in diabetic $ApoE^{-/-}$ mice treated with GKT137831 (Figure 11G). In contrast, MCP-1 protein in renal cortex of diabetic $Nox1^{-/y}ApoE^{-/}$ mice was not different from diabetic $Nox1^{+/y}ApoE^{-/-}$ mice (Figure 11F).

DISCUSSION

This study provides evidence that Nox4-derived, but not Nox1-derived, ROS are causatively linked to the development and progression of diabetic nephropathy. This evidence is based on the first direct comparison of Nox4 or Nox1 deletion in $ApoE^{-/-}$ mice. We used $ApoE^{-/-}$ mice because streptozotocin-induced diabetes in $ApoE^{-/-}$ mice is a well characterized model of advanced renal injury with prominent ECM accumulation.[28,29] Importantly, we translated these findings into a potential clinical therapy by showing that Nox inhibition in diabetic $ApoE^{-/-}$ mice using a pharmacologic strategy resulted in a similar degree of renoprotection to that observed with deletion of Nox4.

Previous studies have already suggested a role for Nox-derived ROS in the development and progression of diabetic nephropathy but these experiments were short term and/or investigated only a single Nox isoform.[4–6,19] With respect to pharmacologic intervention, previous studies relied on nonspecific inhibitors of ROS formation, such as apocynin, a drug that has also been reported to interfere with Rho kinase.[30,31] Therefore, we postulate that this longer-term study is potentially more relevant with respect to clinical target validation.

In this study, we were able to combine observations of a renoprotective effect of genetically deleting Nox4 with pharmacologic inhibition of Nox using the most specific compound currently available, GKT137831. In diabetic $ApoE^{-/-}$ mice, Nox4 deletion or treatment with GKT137831 attenuated various parameters of glomerular injury, including albuminuria, and glomerular structural changes, including ECM accumulation. Furthermore, the diabetes-induced increase in tubulointerstitial area was significantly attenuated using the novel Nox inhibitor GKT137831. In addition, macrophage infiltration was reduced in diabetic Nox4 KO mice and these changes occurred in association with attenuation of the expression of the chemokine MCP-1 and the key proinflammatory transcription factor, NF-κB. In addition, these renoprotective effects were associated with reduced renal cortical superoxide generation and a decrease in both cytosolic and mitochondrial ROS levels as well as reduced nitrotyrosine accumulation within glomeruli. In contrast, genetic deletion of Nox1 in $ApoE^{-/-}$ mice did not attenuate renal ROS generation and failed to prevent glomerular injury in diabetic mice.

Consistent with other studies using type 1 and type 2 diabetic models,[11,12,32] we observed increased Nox4 mRNA in the renal cortex of diabetic mice. One must exert due caution in interpreting results with respect to Nox4 protein expression because there is currently no fully validated monospecific Nox4 antibody available. In the context of

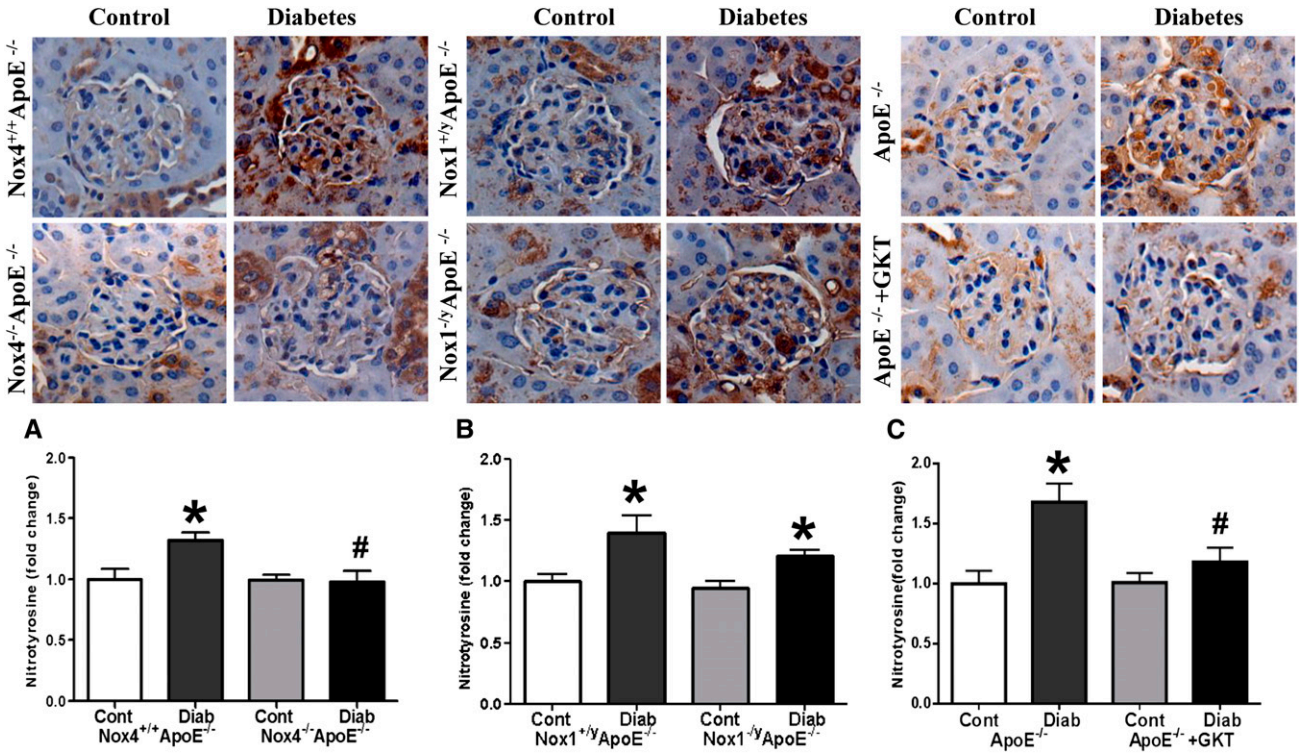

Figure 6. Genetic deficiency of Nox4, but not of Nox1, and pharmacologic Nox inhibition attenuate nitrotyrosine accumulation in glomeruli of diabetic $ApoE^{-/-}$ mice. Immunostaining for nitrotyrosine in glomeruli of control and diabetic $Nox4^{+/+}ApoE^{-/-}$ and $Nox4^{-/-}ApoE^{-/-}$ mice after 20 weeks (A), control and diabetic $Nox1^{+/y}ApoE^{-/-}$ and $Nox1^{-/y}ApoE^{-/-}$ mice after 20 weeks (B), or control and diabetic $ApoE^{-/-}$ mice with and without treatment with GKT137831 for 20 weeks (C) (n=6–8 per group). Results are expressed relative to control $Nox4^{+/+}ApoE^{-/-}$ mice (A), control $Nox1^{+/y}ApoE^{-/-}$ mice (B), or control (untreated) $ApoE^{-/-}$ mice (C), which were arbitrarily assigned a value of 1. Data are the mean±SEM. *P<0.05 versus respective control $Nox4^{+/+}ApoE^{-/-}$ and $Nox4^{-/-}ApoE^{-/-}$ mice (A), control $Nox1^{+/y}ApoE^{-/-}$ and $Nox1^{-/y}ApoE^{-/-}$ mice (B), or control $ApoE^{-/-}$ and $ApoE^{-/-}$ plus GKT137831 mice (C); #P<0.05 versus diabetic $Nox4^{+/+}ApoE^{-/-}$ (A) or diabetic $ApoE^{-/-}$ mice (C). Cont, control; Diab, diabetes; GKT, GKT137831.

these limitations, we identified increased immunoreactivity to Nox4 in diabetic $ApoE^{-/-}$ mice, particularly in the glomerulus, a phenomenon not observed in Nox4 KO mice. These findings are similar to those reported in shorter-term studies by other groups.[19]

A previous study by Gorin *et al.* suggested that short-term downregulation of Nox4 by systemic administration of antisense oligonucleotides attenuated renal and glomerular hypertrophy as well as reduced the increase in fibronectin expression that is commonly seen in the diabetic kidney.[19] This group has recently further explored the link between Nox4 and ECM production and has shown that Nox4 can be modulated by the matrix metalloproteinase, ADAM (a disintegrin and metalloproteinase)-17.[33]

Babelova *et al.*[20] investigated the role of Nox4 in various models of renal injury, including a model of streptozotocin-induced diabetes, albeit in C57BL/6 and not in $ApoE^{-/-}$ mice. Consequently, and in contrast to our findings, those authors did not observe upregulation of Nox4[20] and Nox4 deficiency did not attenuate nephropathy. However, C57BL/6 mice are relatively resistant to the development of typical morphologic features of diabetic nephropathy.[34] These differences in the duration of the experimental model and the mouse strains utilized may explain the conflicting results of that study with our and other studies.[11,19,32]

Given the importance of podocytes not only in albuminuria but also in morphologic manifestations of diabetic nephropathy, and to translate our findings from mice to a human context, we performed *in vitro* studies using human podocytes. In line with the *in vivo* observations using mice, Nox4 and to a lesser extent Nox5 were upregulated in response to high glucose and this upregulation was further amplified in the presence of TGF-β1 exposure, both key features of the diabetic milieu.[35,36] Both silencing of Nox4 and Nox inhibition with GKT137831 reduced ROS levels in human podocytes, and this was associated with attenuation of critical pathways linked to renal fibrosis, including gene expression of collagen IV, fibronectin, connective tissue growth factor, and α-SMA. These findings confirm a previous report in which Nox4 was shown to play an important role in hyperglycemia-induced ROS formation in mouse podocytes[37]; however, our study importantly confirms and extends these findings to human cells and emphasizes the effect of Nox4 on prosclerotic pathways.

The effects of Nox4-derived ROS formation on VEGF expression, a growth factor expressed by renal cells including

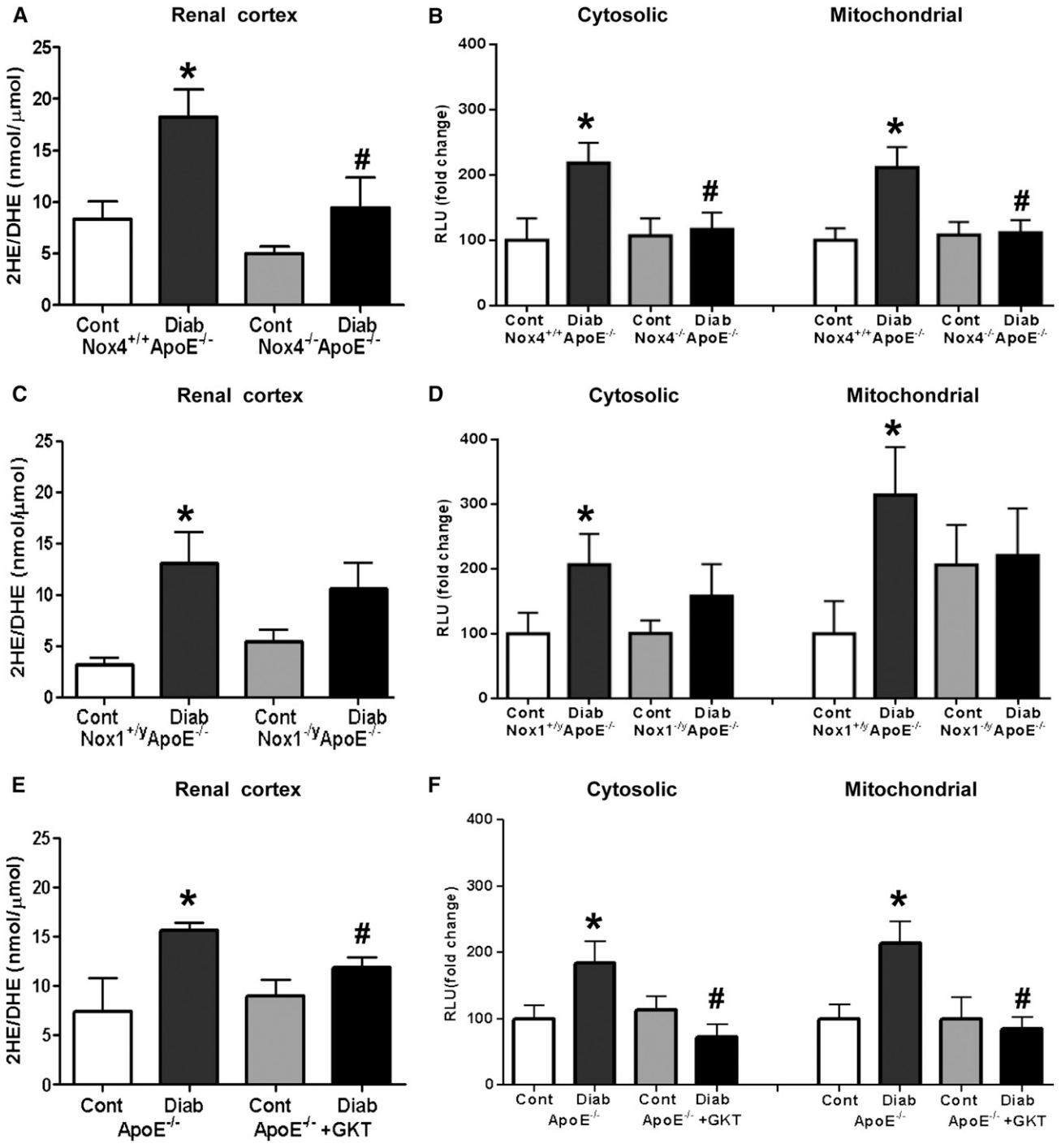

Figure 7. Genetic deficiency of Nox4, but not of Nox1, and pharmacologic Nox inhibition attenuate increased renal superoxide and ROS formation in diabetic $ApoE^{-/-}$ mice. Superoxide production in renal cortex (A, C, and E) and ROS production in cytosolic and mitochondrial fractions of the renal cortex (B, D, and F) in control and diabetic $Nox4^{+/+}ApoE^{-/-}$ and $Nox4^{-/-}ApoE^{-/-}$ mice (A and B), control and diabetic $Nox1^{+/y}ApoE^{-/-}$ and $Nox1^{-/y}ApoE^{-/-}$ mice after 20 weeks (C and D), or control and diabetic $ApoE^{-/-}$ mice with and without treatment with GKT137831 for 20 weeks (E and F) (n=5–6 per group). Superoxide data (A, C, and E) are shown as the ratio of 2HE (nanomoles) to DHE (micromoles). With respect to ROS measurements, results were expressed relative to control $Nox4^{+/+}ApoE^{-/-}$ mice (B), control $Nox1^{+/y}ApoE^{-/-}$ mice (D), or control (untreated) $ApoE^{-/-}$ mice (F), which was arbitrarily assigned a value of 100. Data are the mean±SEM. *$P \leq 0.05$ versus respective control $Nox4^{+/+}ApoE^{-/-}$ or control $Nox1^{+/y}ApoE^{-/-}$ mice or control $ApoE^{-/-}$ mice; $^{\#}P<0.05$ versus diabetic $Nox4^{+/+}ApoE^{-/-}$ or diabetic $ApoE^{-/-}$ mice. 2HE, 2 hydroethidium; Cont, control; Diab, diabetes; DHE, dihydroethidium; GKT, GKT137831; RLU, relative light unit.

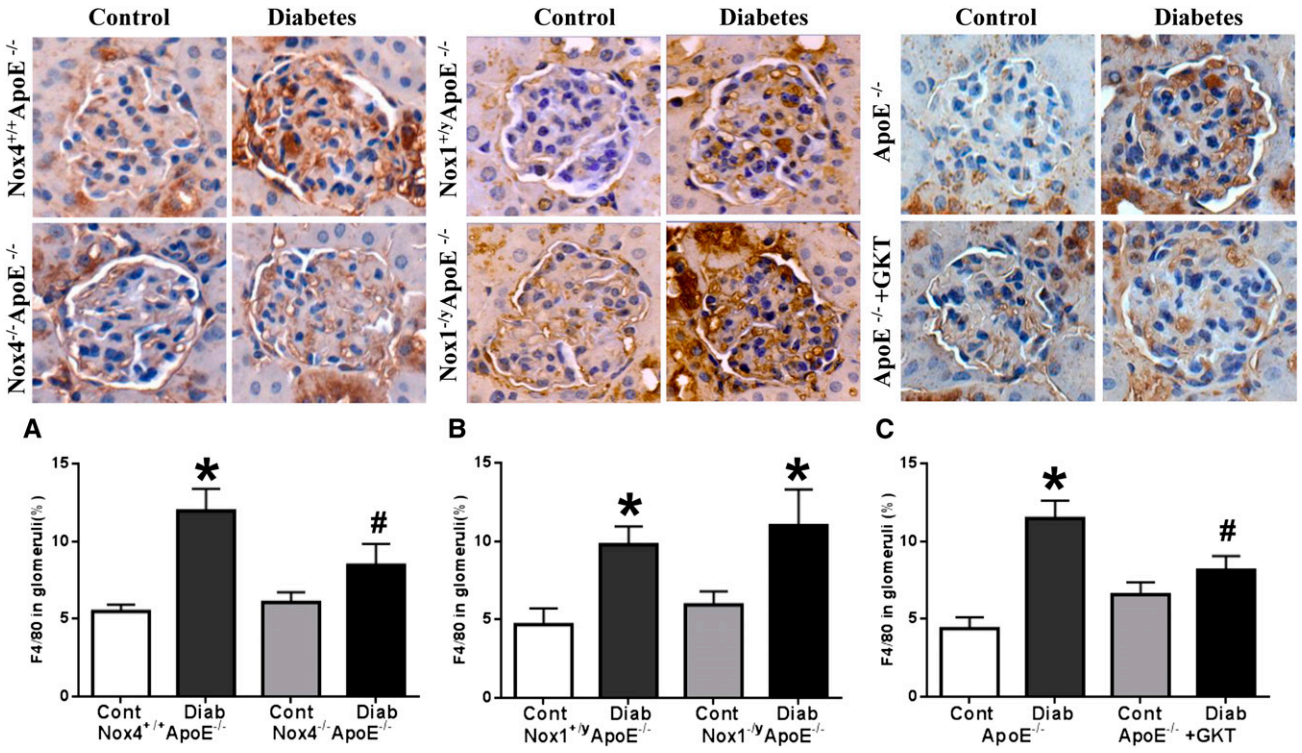

Figure 8. Genetic deficiency of Nox4, but not of Nox1, and pharmacologic Nox inhibition attenuates macrophage infiltration in glomeruli of diabetic *ApoE*$^{-/-}$ mice. Immunostaining for F4/80 in glomeruli of control and diabetic *Nox4*$^{+/+}$*ApoE*$^{-/-}$ and *Nox4*$^{-/-}$ *ApoE*$^{-/-}$ mice (A) or in control and diabetic *Nox1*$^{+/y}$*ApoE*$^{-/-}$ and *Nox1*$^{-/y}$*ApoE*$^{-/-}$ mice after 20 weeks (B), or control and diabetic *ApoE*$^{-/-}$ mice with and without treatment with GKT137831 for 20 weeks (C) (n=6–8 per group). Data are the mean±SEM. *P<0.05 versus respective control *Nox4*$^{+/+}$*ApoE*$^{-/-}$ and *Nox4*$^{-/-}$*ApoE*$^{-/-}$ mice (A), control *Nox1*$^{+/y}$*ApoE*$^{-/-}$ and *Nox1*$^{-/y}$*ApoE*$^{-/-}$ mice (B), or control *ApoE*$^{-/-}$ and *ApoE*$^{-/-}$ plus GKT137831 mice (C); $^{\#}P$<0.05 versus diabetic *Nox4*$^{+/+}$*ApoE*$^{-/-}$ (A) or diabetic *ApoE*$^{-/-}$ mice (C). Cont, control; Diab, diabetes; GKT, GKT137831.

podocytes,[38] were also confirmed by our *in vivo* studies of diabetic nephropathy. Both Nox4 deletion and inhibition of Nox with GKT137831 were associated with attenuation of the diabetes-induced increase in VEGF expression in glomeruli, and this was also associated with reduced proteinuria. Furthermore, in our *in vitro* studies, GKT137831 treatment attenuated podocyte VEGF expression in a hyperglycemic milieu. Importantly, this is likely to be Nox4 dependent because downregulation of Nox4 in human podocytes was also associated with attenuation of VEGF expression. Consistent with our findings, other researchers reported a link between VEGF with Nox4 in the retina, where Nox4 was associated with vascular permeability,[39] as well as similar findings in a stroke model.[40]

Diabetic nephropathy is considered to be at least in part an inflammatory disorder in which progressive glomerular injury is associated with macrophage infiltration.[25] Consistent with this view, induction of diabetes in our study was associated with a significant increase in accumulation of macrophages within the glomeruli. These changes were attenuated in diabetic Nox4-deficient mice and in diabetic *ApoE*$^{-/-}$ mice treated with the Nox inhibitor GKT137831 but not in diabetic *Nox1*$^{-/y}$ mice. A link between Nox4 and inflammation was previously suggested, albeit in a nonrenal context. Specifically, Nox4 downregulation using a small interfering RNA approach attenuated the LPS-induced proinflammatory response in human endothelial cells.[41] Consistent with these effects of Nox4 deletion on renal macrophage infiltration, we observed reduced expression of the key proinflammatory transcription factor NF-κB as well as the well characterized NF-κB–dependent chemokine MCP-1 on the gene and protein level in the renal cortex. Complementary *in vitro* studies in human podocytes confirmed that high glucose–induced upregulation of the NF-κB subunit, p65, and MCP-1 could be prevented by silencing of Nox4.

Block *et al.* suggested that Nox4 is present in the mitochondria, and that silencing of mitochondrial Nox4 is associated with reduced mitochondrial oxidative stress and injury.[15] Thus, we examined ROS formation in not only the cytosolic fraction but also in the mitochondrial fraction of the renal cortex. Indeed, we demonstrated reduced mitochondrial as well as cytosolic ROS generation in the renal cortex of diabetic Nox4-deficient mice. GKT137831 treatment of diabetic *ApoE*$^{-/-}$ mice caused similar reductions in mitochondrial ROS

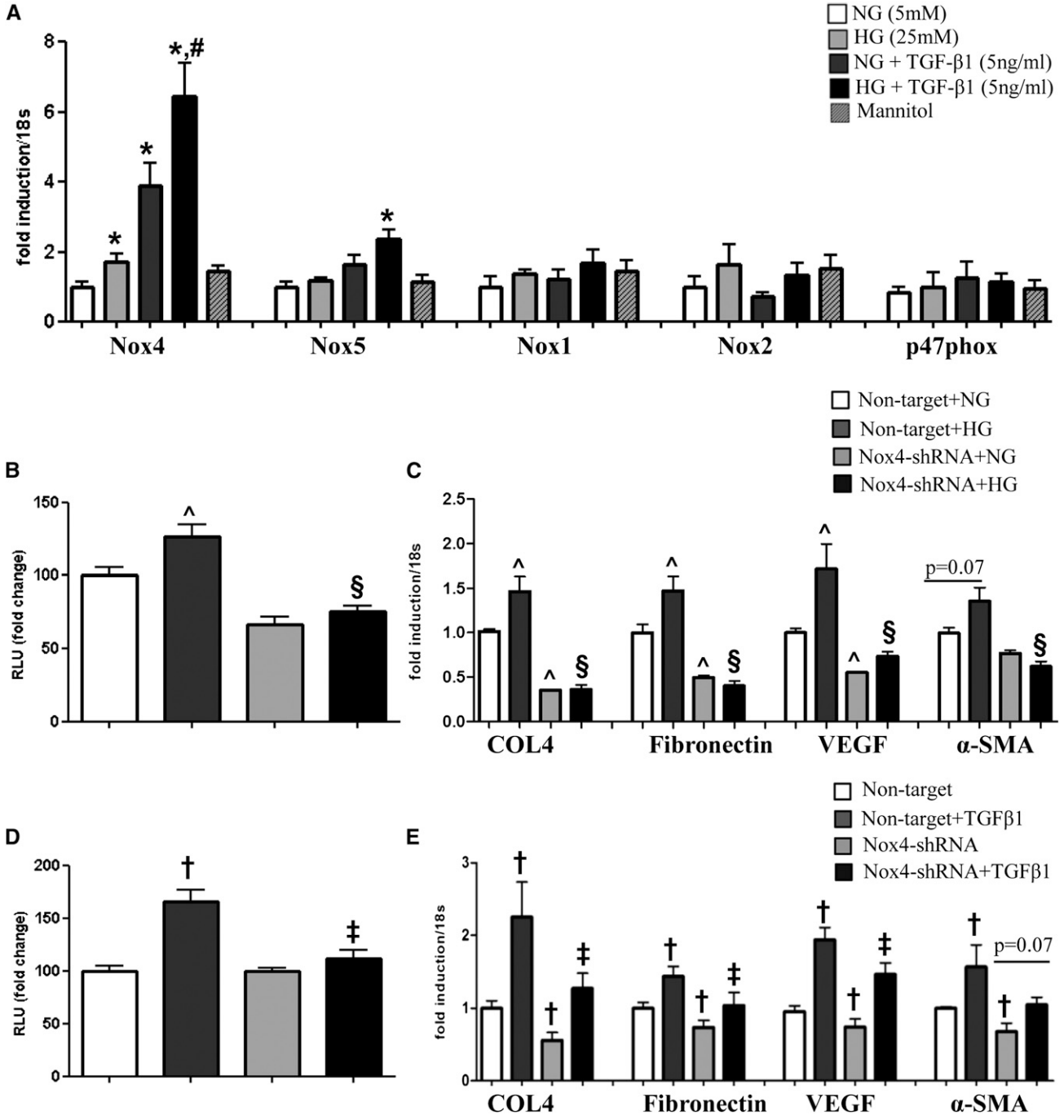

Figure 9. Silencing of Nox4 attenuates high glucose–as well as high glucose plus TGF-β1–mediated ROS formation and gene expression of profibrotic markers in human podocytes. (A) Nox4 and Nox5, but not Nox1, Nox2, or p47phox mRNA levels were upregulated in human podocytes by diabetic stimuli. Analysis of Nox isoform mRNA levels and the cytosolic regulator, p47phox, in cultured differentiated human podocytes in NG (5 mM) or HG (25 mM) and in the presence or absence of TGF-β1 (5 ng/ml, 2 days). Mannitol (20 mM/L+5 mM D-glucose) served as an osmotic control. Data are the mean±SEM. *$P<0.05$ versus NG; $^{\#}P<0.05$ versus HG. (B and C) Analysis of ROS production (B) and RT-PCR (C) for collagen IV, fibronectin, VEGF and α-SMA in differentiated human podocytes transfected with shRNA specific for Nox4 and then grown in NG (5 mM) or HG (25 mM) for 2 days (B and C). Results for ROS production are expressed relative to nontarget plus NG, which was arbitrarily assigned a value of 100 (B). Data are the mean±SEM (n=6/group). $^{\wedge}P<0.05$ versus nontarget plus NG; $^{\S}P<0.05$ versus nontarget plus HG. (D and E) Analysis of ROS production (D) and RT-PCR (E) for collagen IV, fibronectin, VEGF and α-SMA in differentiated human podocytes transfected with shRNA specific for Nox4 and then grown in the presence or absence of TGF-β1 (5 ng/ml) for 4 hours for ROS production (D) and 2days for RT-PCR (E). Data are the mean±SEM (n=6/group). $^{\dagger}P<0.05$ versus nontarget, $^{\ddagger}P<0.05$ versus non-target plus TGF-β1. HG, high glucose; NG, normal glucose; RLU, relative light unit.

generation. These findings strengthen the view that Nox4 is not only a cytosolic but also a mitochondrial source of ROS, at least in the diabetic kidney. Other groups have shown that alterations in the electron transport chain are a major source of mitochondrial ROS in the setting of hyperglycemia.[42,43] However, our findings extend these results by demonstrating that Nox4 may be an alternative or additional target to reduce mitochondrial oxidative stress, particularly in the kidney.

The role of Nox1 in diabetic nephropathy has not been clearly delineated previously. Nox1 is expressed in the renal cortex, including in glomeruli of the normal kidney, albeit at almost undetectable levels. Increased renal expression of Nox1 has been reported in hypertension-associated forms of renal disease such as in models of angiotensin II infusion and in Dahl salt-sensitive hypertensive rats.[44,45] These findings are relevant because activation of the renin-angiotensin system in the diabetic kidney has been shown to promote renal injury.[46,47] Angiotensin II induces upregulation of Nox1.[48] Therefore, it has been postulated that Nox1 could play an important role in the development and progression of diabetic nephropathy.[44,45] However, in our study, Nox1 deletion was not associated with an improvement in diabetes-related renal injury. Thus, our findings argue against a critical role for Nox1 in diabetic nephropathy but Nox1 may be more important, as recently suggested, in diabetes-associated macrovascular disease.[49]

We focused our study on Nox1 and Nox4 and did not specifically address Nox2, which was previously shown to not play a key role in diabetic nephropathy.[50] Furthermore, Nox2 deletion was reported to be associated with increased susceptibility to infections in the context of diabetes mellitus.[14] Nevertheless, one cannot exclude a potential role for partial Nox2 inhibition but the lethality of severe Nox2 deficiency in hyperglycemic states is likely to narrow the therapeutic window of such an approach. There are also increasing data to suggest a role for another Nox isoform, Nox5, in pathologic ROS generation.[7,51] However, because Nox5 is not present in rats and mice, we were not able to delineate the contribution of this particular Nox isoform in our *in vivo* models. Nevertheless, in human podocytes, Nox5 was upregulated upon treatment with diabetes-related stimuli, such as high glucose and TGF-β1. Thus, we cannot exclude an additional role for Nox5 in human diabetic nephropathy.

To test the possibility to clinically translate our experimental studies, we administered GKT137831 to diabetic $ApoE^{-/-}$ mice. This Nox inhibitor has been suggested to have dual efficacy on Nox1 and Nox4. It has been shown to provide end-organ protective effects, albeit in the liver.[22,52] Importantly, in our study, treatment of diabetic $ApoE^{-/-}$ mice with GKT137831 mimicked the effects of Nox4 deletion on glomerular injury, albuminuria, ROS production, ECM accumulation, and macrophage infiltration. Thus, the renoprotective effects of GKT137831 are likely to be mediated by Nox4 rather than Nox1 inhibition. In line with our study results, another Nox inhibitor, GKT136901, was recently reported to be renoprotective in a model of type 2 diabetes, the db/db mouse. This renoprotective effect was associated with reduced albuminuria and urinary excretion of thiobarbituric acid–reactive substances as well as attenuation of renal extracellular signal-regulated protein kinase 1/2 phosphorylation.[8] The initial antialbuminuric effect observed in that study was not sustained after 16 weeks of diabetes. It is possible that the longer lasting antialbuminuric effect seen in our study may be related to a difference in potency between the two compounds or more likely related to the mode of administration of the Nox inhibitor. The drug was mixed in the food in the previous study,[8] whereas the drug was administered by gavage in this study.

In conclusion, compelling evidence is provided that Nox4, but not Nox1, is a major pathologic renal source of ROS in a long-term model of insulin-deficient diabetes leading to relatively advanced diabetic nephropathy. Our experiments have identified Nox4 as an attractive mechanism-based therapeutic target for the treatment of diabetic nephropathy. Furthermore, we provide proof of principle that this mechanism can be translated into a novel pharmacologic therapy with important future clinical implications. Therefore, our study strengthens the need to develop Nox4-specific inhibitors that can be used for prevention and treatment of this major diabetic complication.

CONCISE METHODS

Animals

Diabetes-induced renal functional changes and morphologic kidney damage were studied in diabetic $Nox4^{+/+}ApoE^{-/-}$, $Nox4^{-/-}ApoE^{-/-}$ double KO, $Nox1^{+/y}ApoE^{-/-}$, $Nox1^{-/y}ApoE^{-/-}$ double KO, and $ApoE^{-/-}$ male mice and compared with respective nondiabetic control mice. $Nox1^{+/y}ApoE^{-/}$ mice were generated as previously described.[53,54] To generate the double KO mice, Nox4 KO mice[41] were crossed for 10 generations with the $ApoE^{-/-}$ mouse strain (Animal Resources Centre, Murdoch, WA, Australia). Initially we mated $ApoE^{-/-}$ (F) with $Nox4^{-/-}$ (M) mice to produce heterozygotes in the F1 generation ($Nox4^{+/-}ApoE^{+/-}$). From the F2 generation we set up $Nox4^{+/-}$ $ApoE^{-/-}$ × $Nox4^{-/-}ApoE^{+/-}$ and $Nox4^{-/-}ApoE^{+/-}$ × $Nox4^{-/-}ApoE^{-/-}$, which produced the F3 generation including the WT $Nox4^{+/+}ApoE^{-/-}$ and double KO $Nox4^{-/-}ApoE^{-/-}$ mice. From that generation, we mated male and female $Nox4^{-/-}$ $ApoE^{-/-}$ mice and are now at the 16th generation.

Diabetes was induced in 6-week-old mice by five daily intraperitoneal injections of streptozotocin (Sigma-Aldrich, St Louis, MO), at a dose of 55 mg/kg in citrate buffer, with control mice receiving citrate buffer alone. None of the animals with diabetes required supplemental insulin to maintain body weight or to prevent ketosis. A subgroup of diabetic and nondiabetic $ApoE^{-/-}$ mice were treated with the Nox inhibitor, GKT137831, administered daily by gavage at a dose of 60 mg/kg per day for 20 weeks commencing with the last injection of streptozotocin. GKT137831, a member of the pyrazolopyridinedione family, is a specific inhibitor of both Nox4 and Nox1 isoforms (K_i in the range of 100–150 nM in cell-free assays of ROS production). It has no ROS scavenging activity when tested at a concentration of 10 μM.[52,55]

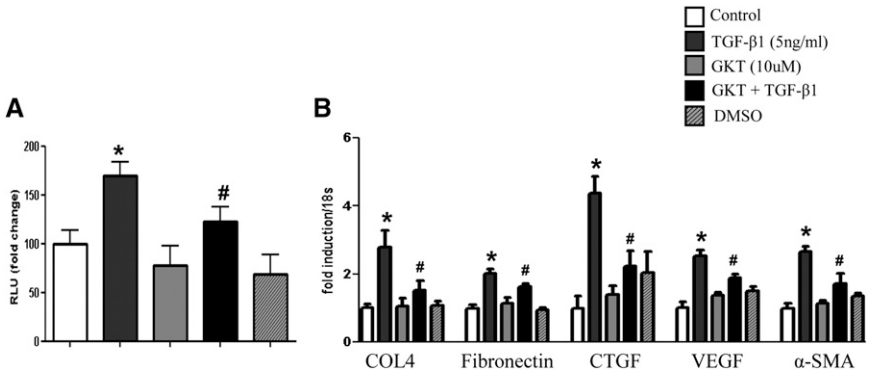

Figure 10. Nox inhibition ameliorates TGF-β1–induced ROS generation and gene expression of profibrotic markers in human podocytes. (A) Nox inhibition ameliorates TGF-β1–induced ROS generation in human podocytes. Analysis of ROS production in cultured differentiated human podocytes after pretreatment with and without GKT137831 (10 μM) for 2 hours in the presence and absence of TGF-β1 (5 ng/ml) for 4 hours. DMSO serves as the vehicle control. Results are expressed relative to control, which is arbitrarily assigned a value of 100. (B) Nox inhibition decreases the high glucose– and TGF-β1–induced increased gene expression of collagen IV, fibronectin, CTGF, VEGF, and α-SMA in human podocytes. The mRNA levels are quantified in cultured differentiated human podocytes after pretreatment with and without GKT137831 (10 μM) for 2 hours in the presence or absence of TGF-β1 (5 ng/ml) for 2 days. DMSO serves as the vehicle control. Data are the mean±SEM (n=6 per group). *P<0.05 versus control; #P<0.05 versus TGF-β1. COL4, collagen IV; CTGF, connective tissue growth factor; GKT, GKT137831; RLU, relative light unit.

After 20 weeks, animals were anesthetized by sodium pentobarbitone intraperitoneally (100 mg/kg body weight) (Euthatal; Sigma-Aldrich, Castle Hill, NSW, Australia). The kidneys were rapidly dissected, weighed, and snap-frozen or processed to paraffin for subsequent analysis. All animal studies were approved by the Alfred Medical Research & Education Precinct Animal Ethics Committee under guidelines of the National Health and Medical Research Council of Australia. All animals were housed at the Precinct Animal Centre of the Baker IDI Heart & Diabetes Institute. During the study, animals had unrestricted access to water and food and were maintained on a 12-hour light/dark cycle in a pathogen-free environment on standard mouse chow (Specialty Feeds, Perth, WA, Australia).

Measurement of Metabolic Parameters

At 10 and 20 weeks after induction of diabetes, mice were placed individually into metabolic cages (Iffa Credo, L'Arbresele, France) for 24 hours. Urine was collected for subsequent analysis. Blood glucose was measured serially using a glucometer (Accutrend; Boehringer Manheim Biochemica, Manheim, Germany). Glycated hemoglobin was measured by HPLC (CLC330 GHb Analyzer; Primus, Kansas City, MO) in lysates of erythrocytes separated from whole blood.[56] Systolic BP was assessed using a computerized noninvasive tail-cuff method.[57] Mice were familiarized with the equipment with readings taken by an experienced technician in conscious mice at the end of the 20-week study. Urinary albumin concentration was measured at 10 and 20 weeks after the induction of diabetes, using a mouse albumin ELISA quantitation kit (Bethyl Laboratories, Montgomery, TX). Urinary creatinine concentrations were measured by HPLC as previously described.[56,58] The urinary albumin/creatinine ratios were calculated.

In Vivo Gene Expression Analyses

Total RNA was extracted after homogenizing renal cortex (Polytron PT-MR2100; Kinematicca, Littau/Lucerne, Switzerland) in TRIzol reagent (Invitrogen Australia, Mt Waverly, VIC, Australia) as previously described.[56] Gene expression using probes and primers as described in Supplemental Table 1 for Nox1, Nox2, Nox4, MCP-1, and NF-κB p65 were analyzed quantitatively and relative to the expression the housekeeping gene 18S (18S ribosomal RNA TaqMan Control Reagent kit) using the TaqMan system (ABI Prism 7500; PerkinElmer, Poster City, CA).[14,56] Results were expressed relative to nondiabetic ApoE$^{-/-}$ mice, which were arbitrarily assigned a value of 1.

Histologic Assessment

Three-micrometer kidney sections were stained with periodic acid–Schiff for measurement of glomerulosclerotic injury and mesangial expansion. Mesangial area was analyzed (percentage of glomerular area) from digital pictures of glomeruli (20 glomeruli per kidney per animal) using Image-Pro plus 6.0 software (Media Cybernetics, Bethesda, MD), as previously described.[56,58] Glomerulosclerotic injury was graded based on the severity of glomerular damage, including mesangial matrix expansion, hyalinosis with focal adhesion, capillary dilation, glomerular tuft occlusion, and sclerosis, as previously described.[12,29,59] Twenty glomeruli per kidney were assessed in a blinded fashion.

Immunohistochemistry

Renal paraffin sections (4-μm) were stained for collagen IV (1:600, rabbit polyclonal anti-collagen IV; Abcam, Cambridge, MA), fibronectin (1:800, polyclonal rabbit anti-fibronectin; Dako Cytomation, Glostrup, Denmark), nitrotyrosine (1:100, rabbit polyclonal anti-nitrotyrosine; Millipore, Billerica, MA), F4/80 (1:50, rat monoclonal anti- F4/80; Abcam) and VEGF (mouse monoclonal anti-human VEGF; Millipore, Upstate Biotechnology, Lake Placid, NY). Briefly, sections were dewaxed, hydrated, and quenched with 3% H_2O_2 in Tris-buffered saline (TBS) to inhibit endogenous peroxidase activity. Sections for collagen IV and fibronectin were digested with 0.4% pepsin (Sigma-Aldrich) in 0.01 M HCl at 37°C. This was followed by incubation with 0.5% milk diluted in TBS to block nonspecific binding. Subsequently, sections were incubated with the primary antibody overnight at 4°C followed by avidin/biotin blocking. Sections for nitrotyrosine were incubated with 10% normal horse serum in TBS instead of 0.5% milk before incubation with the primary antibody. Similarly, sections for F4/80 were incubated with protein blocking agent (Dako CSA Kit) before incubation with the primary

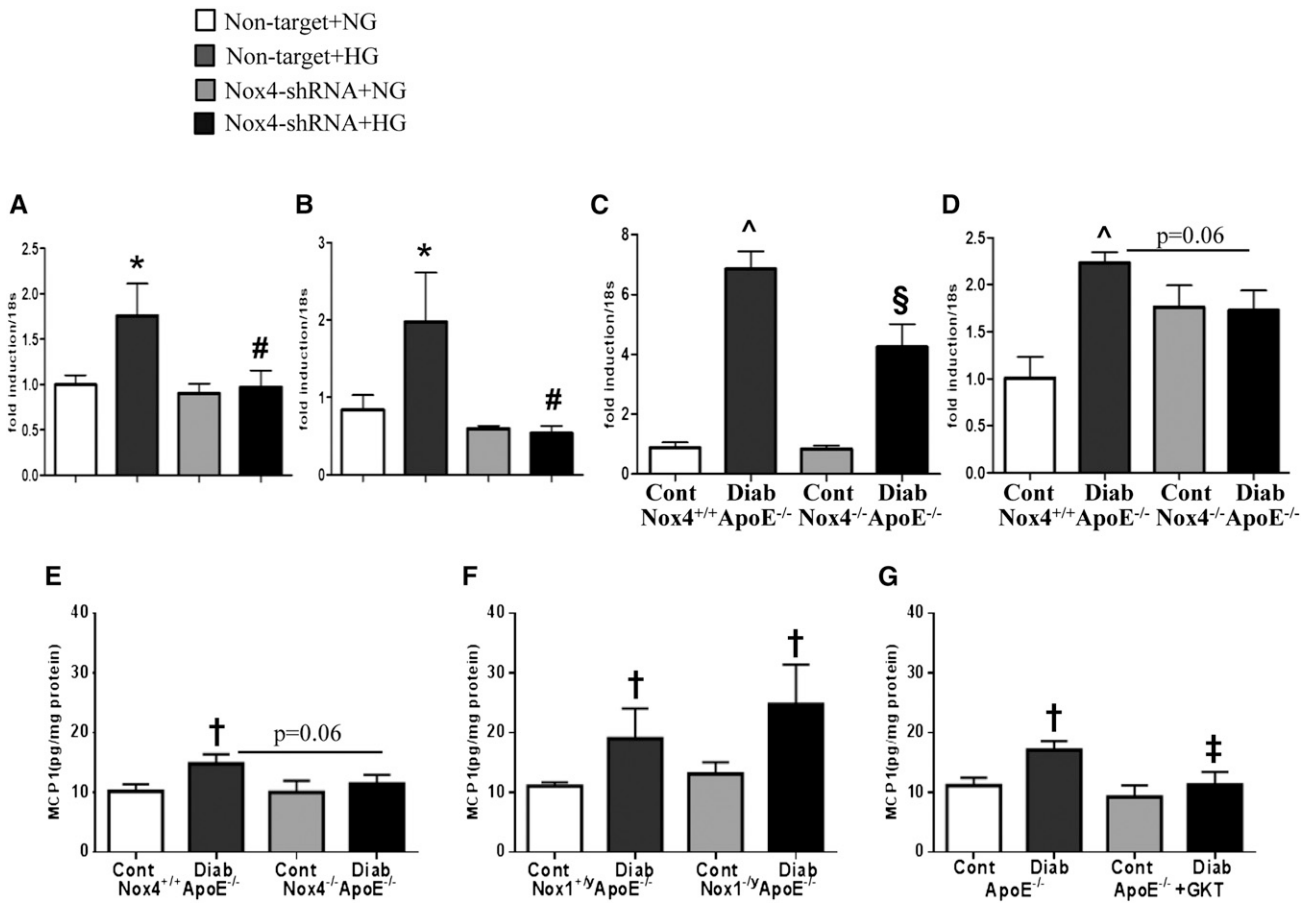

Figure 11. Genetic targeting of Nox4 attenuates diabetes-induced increased expression of proinflammatory markers MCP-1 and NF-κB p65 *in vitro* and *in vivo*. (A and B) RT-PCR analysis of (A) MCP-1 and (B) NF-κB p65 in human podocytes transfected with shRNA specific for Nox4 and then grown in NG (5 mM) or HG (25 mM) for 2 days. Data are the mean±SEM (n=6/group). *P<0.05 versus nontarget plus NG; #P<0.01 versus nontarget plus HG. (C and D) RT-PCR analysis of (C) MCP-1 and (D) NF-κB p65 in renal cortex of control and diabetic $Nox4^{+/+}ApoE^{-/-}$ and $Nox4^{-/-}ApoE^{-/-}$ mice after 20 weeks. Data are the mean±SEM (n=6/group). ^P<0.05 versus control $Nox4^{+/+}ApoE^{-/-}$; §P<0.05 versus diabetic $Nox4^{+/+}ApoE^{-/-}$ mice. (E and F) Measurement of MCP-1 by ELISA in protein extracts of renal cortex of (E) control and diabetic $Nox4^{+/+}ApoE^{-/-}$ and $Nox4^{-/-}ApoE^{-/-}$ mice or in (F) control and diabetic $Nox1^{+/y}ApoE^{-/-}$ and $Nox1^{-/y}ApoE^{-/-}$ mice after 20 weeks, (n=5–6/group) or in (G) control and diabetic $ApoE^{-/-}$ mice with and without treatment with *GKT137831* for 20 weeks, (n=5–6/group). Data are the mean±SEM. †P<0.05 versus respective control $Nox4^{+/+}ApoE^{-/-}$ and $Nox4^{-/-}ApoE^{-/-}$ mice (E) or control $Nox1^{+/y}ApoE^{-/-}$ and $Nox1^{-/y}ApoE^{-/-}$ mice (F) or control $ApoE^{-/-}$ and $ApoE^{-/-}$ plus GKT137831 mice (G); ‡P<0.05 versus diabetic $ApoE^{-/-}$ mice (G). Cont, control; Diab, diabetes; GKT, GKT137831; HG, high glucose; NG, normal glucose.

antibody anti-F4/80 overnight at 4°C and staining was also amplified further by Dako Catalyzed Signal Amplification Kit, according to the manufacturer's instructions. Thereafter, biotinylated anti-rabbit Ig (1:500) for collagen IV, fibronectin, nitrotyrosine, and biotinylated anti-rat Ig (1:200) for F4/80 (Vector Laboratories, Burlingame, CA) were applied as the secondary antibody, followed by horseradish peroxidase–conjugated streptavidin (VECTASTAIN Elite ABC Staining Kit; Vector Laboratories). Peroxidase conjugates were subsequently visualized using 3,3′-diaminobenzidine tetrahydrochloride (Sigma-Aldrich) in 0.08% H_2O_2/TBS. For VEGF immunostaining, a Dako ARK Peroxidase for Mouse Primary Antibodies protocol was followed. Sections were dewaxed, hydrated, and incubated with peroxidase block followed by incubation with biotinylated primary anti-VEGF antibody for 1 hour at room temperature and incubation with streptavidin peroxidase. Peroxidase conjugates were subsequently visualized using 3,3′-diaminobenzidine substrate chromogen.

Finally, sections were counterstained with Mayer's hematoxylin, dehydrated, and mounted. All sections were examined under a light microscope (Olympus BX-50; Olympus Optical, Tokyo, Japan) and digitized with a high-resolution camera. For the quantification of the proportional area of staining, 20 glomeruli (×400) were analyzed using Image-Pro plus 6 (Media Cybernetics).[56,58] All assessments were performed in a blinded manner. Six or eight kidneys were investigated in each group.

MCP-1 ELISA

The concentration of MCP-1 was identified in the protein extracts obtained from the renal cortex for each group (n=5–6 per group) by

using the instructions of an ELISA kit (1:3; R&D Systems, Kirrawee, NSW, Australia). The ELISA results were expressed relative to the protein concentration.

Measurements of Superoxide and ROS Production in Renal Cortex

Renal superoxide levels were measured in frozen kidney cortex using HPLC calibrated to measure dihydroethidium by a previously established method.[14,24] Furthermore, ROS levels were measured in frozen kidney cortex. Briefly, renal cortex was homogenized in Krebs buffer, and cytosolic and mitochondrial fractions were prepared by differential centrifugation as previously described.[24] Cytosolic and mitochondrial isolates were assayed in duplicate in clear 96-well plates and prewarmed Krebs-HEPES supplemented with L-012 (Wako Chemicals, Richmond, VA) at a concentration of 100 μM added to each well in the dark and incubated at 37°C for 10 minutes. After incubation, plates were read in a luminometer (MicroLumat Plus; Berthold Technologies, Pforzheim, Germany) and luminescence was measured with a single measuring time of 1 second and cycle time of 111 seconds for 20 minutes at 37°C. Buffer blank was subtracted from each reading. A bicinchoninic acid protein assay (Pierce/Thermo Scientific, Scoresby, VIC, Australia) was performed (samples 1:10 in PBS) according to the kit instructions and results were expressed relative to the total protein concentration (in milligrams).

In Vitro Experiments

Conditionally immortalized human podocytes were used for the *in vitro* study.[60] Podocytes were grown in RPMI with 10% FCS and 1× ITS media supplement (Sigma-Aldrich), which contains 1.0 mg/ml insulin from bovine pancreas, 0.55 mg/ml human transferrin, and 0.5 μg/ml sodium selenite in a humidified incubator, 5% CO_2 at 33°C. Approximately 60% confluent cells were transferred to 2% FBS media and incubated at 37°C for 2 weeks.[27] Under these conditions, the podocytes undergo growth arrest, display the typical arborized pattern of foot process extensions (Supplemental Figure 3), and express markers of mature podocytic differentiation *in vivo*, including Wilms' tumor-1 and nephrin (Supplemental Figure 4). Cells were then cultured in RPMI with 5 mmol/L glucose or 25 mmol/L glucose in the presence or absence of TGF-β1 (5 ng/ml; R&D Systems, Minneapolis, MN) with or without GKT137831 (10 μM) dissolved in 0.1% DMSO and incubated for 48 hours at 37°C.

shRNA to Nox4

The knockdown of Nox4 was performed in human podocyte using MISSION shRNA expressing lentivirus vectors (Sigma-Aldrich) as previously described.[61] The sequence targeting Nox4 knockdown corresponds to 5′-GCTGTATATTGATGGTCCTTT-3′ (TRCN0000046089). Cells transduced with the MISSION nontarget shRNA control vector particles (Sigma-Aldrich) were used as controls. The undifferentiated podocytes were seeded at 1×10^6 cells per dish in a 100-mm dish and infected by the lentivirus particles in the presence of 8 μg/ml polybrene, followed by selection in puromycin (1 μg/ml; Sigma-Aldrich) for 4 days. The knockdown efficiency in the cells was verified by RT-PCR and was approximately 70% for Nox4. Nontarget and Nox4-shRNA–infected cells were then cultured in RPMI with 5 mmol/L glucose or 25 mmol/L glucose or in the presence or absence of TGF-β1 (5 ng/ml) and incubated for 48 hours at 37°C. At the end of each experiment, cells were harvested and RNA was extracted by the TRIzol method and cDNA was synthesized for quantitative RT-PCR.

In Vitro Gene Expression Analyses

Gene expression was analyzed by real-time RT-PCR, using the TaqMan system based on real-time detection of accumulated fluorescence (ABI Prism 7500; PerkinElmer). Fluorescence for each cycle was quantitatively analyzed by an ABI Prism 7500 Sequence Detection System (PerkinElmer). To control for variation in the amount of DNA that was available for PCR in the different samples, gene expression of the target sequence was normalized in relation to the expression of an endogenous control 18S ribosomal RNA (18S rRNA TaqMan Control Reagent Kit, ABI Prism 7500; PerkinElmer). Triplicate experiments were performed, with six replicates each. Results were expressed relative to control (untreated) cells, which was arbitrarily assigned a value of 1. Human probe and primer sequences used for quantitative RT-PCR are shown in Supplemental Table 2.

Measurement of ROS *In Vitro*

Fully differentiated normal, nontarget, and Nox4-shRNA infected human podocytes were trypsinized and resuspended in 200 μl RPMI media at a density of 10^4 cells per well of a white 96-well microplate (PerkinElmer) and incubated at 37°C for 24 hours. Normal human podocytes were then cultured with or without GKT137831 (10 μM) for 2 hours and then treated with or without TGF-β1 (5 ng/ml) for 4 hours at 37°C. However, nontarget and Nox4-shRNA–infected cells were cultured in normal glucose (5 mM) or in high glucose (25 mM) for 2 days or in the presence or absence of TGF-β1 (5 ng/ml) for 4 hours at 37°C. Each well was washed with Krebs-HEPES, and 100 μl of Krebs-HEPES supplemented with L-012 (100 μM) (Wako Chemicals) was subsequently added and incubated at 37°C for 10 minutes. After incubation, plates were read on a luminometer (Berthold Technologies).

Statistical Analyses

All parameters were analyzed by one-way ANOVA using GraphPad Prism 5 software (GraphPad Software, Inc., La Jolla, CA) for multiple comparisons of the means or analyzed by the two-tailed unpaired Mann–Whitney *U* test when required. A P value<0.05 was considered statistically significant. Results are expressed as the mean±SEM, unless otherwise specified.

ACKNOWLEDGMENTS

The authors thank Dr. Ying He (Ottawa Hospital Research Institute, Ottawa, ON, Canada) and Edward Grixti, Maryann Arnstein, Kylie Gilbert, Jade Mosele, and Laura van Banning (Baker IDI Heart & Diabetes Institute, Melbourne, Australia) for experimental animal handling and technical support.

This work was supported by grants from the National Health & Medical Research Council (NHMRC) of Australia, the Juvenile Diabetes Research Foundation (JDRF), the Diabetes Australia Research

Trust, and the FP7 Framework Programme. K.A.J.-D. is supported by a NHMRC Senior Research Fellowship. M.E.C. is an Australian Fellow for the NHMRC and a recipient of a JDRF Scholars Award. H.H.H.W.S. is supported by a Marie Curie International reintegration grant, a European Research Council advanced investigator grant, and the Dutch Kidney Foundation. R.M.T. was supported by a Canada Research Chair/Canadian Institutes of Health Research/Canadian Foundation for Innovation award.

DISCLOSURES

C.S. and F.H. are paid employees and own shares of Genkyotex SA, Geneva, Switzerland.

REFERENCES

1. Molitch ME, DeFronzo RA, Franz MJ, Keane WF, Mogensen CE, Parving HH, Steffes MW; American Diabetes Association: Nephropathy in diabetes. *Diabetes Care* 27[Suppl 1]: S79–S83, 2004
2. Calcutt NA, Cooper ME, Kern TS, Schmidt AM: Therapies for hyperglycaemia-induced diabetic complications: From animal models to clinical trials. *Nat Rev Drug Discov* 8: 417–429, 2009
3. Kakehi T, Yabe-Nishimura C: NOX enzymes and diabetic complications. *Semin Immunopathol* 30: 301–314, 2008
4. Kitada M, Koya D, Sugimoto T, Isono M, Araki S, Kashiwagi A, Haneda M: Translocation of glomerular p47phox and p67phox by protein kinase C-beta activation is required for oxidative stress in diabetic nephropathy. *Diabetes* 52: 2603–2614, 2003
5. Satoh M, Fujimoto S, Haruna Y, Arakawa S, Horike H, Komai N, Sasaki T, Tsujioka K, Makino H, Kashihara N: NAD(P)H oxidase and uncoupled nitric oxide synthase are major sources of glomerular superoxide in rats with experimental diabetic nephropathy. *Am J Physiol Renal Physiol* 288: F1144–F1152, 2005
6. Susztak K, Raff AC, Schiffer M, Böttinger EP: Glucose-induced reactive oxygen species cause apoptosis of podocytes and podocyte depletion at the onset of diabetic nephropathy. *Diabetes* 55: 225–233, 2006
7. Sedeek M, Hébert RL, Kennedy CR, Burns KD, Touyz RM: Molecular mechanisms of hypertension: Role of Nox family NADPH oxidases. *Curr Opin Nephrol Hypertens* 18: 122–127, 2009
8. Sedeek M, Gutsol A, Montezano AC, Burger D, Nguyen Dinh Cat A, Kennedy CR, Burns KD, Cooper ME, Jandeleit-Dahm K, Page P, Szyndralewiez C, Heitz F, Hebert RL, Touyz RM: Renoprotective effects of a novel Nox1/4 inhibitor in a mouse model of Type 2 diabetes. *Clin Sci (Lond)* 124: 191–202, 2013
9. Selemidis S, Sobey CG, Wingler K, Schmidt HH, Drummond GR: NADPH oxidases in the vasculature: Molecular features, roles in disease and pharmacological inhibition. *Pharmacol Ther* 120: 254–291, 2008
10. Wingler K, Hermans JJ, Schiffers P, Moens A, Paul M, Schmidt HH: NOX1, 2, 4, 5: Counting out oxidative stress. *Br J Pharmacol* 164: 866–883, 2011
11. Etoh T, Inoguchi T, Kakimoto M, Sonoda N, Kobayashi K, Kuroda J, Sumimoto H, Nawata H: Increased expression of NAD(P)H oxidase subunits, NOX4 and p22phox, in the kidney of streptozotocin-induced diabetic rats and its reversibity by interventive insulin treatment. *Diabetologia* 46: 1428–1437, 2003
12. Giunti S, Calkin AC, Forbes JM, Allen TJ, Thomas MC, Cooper ME, Jandeleit-Dahm KA: The pleiotropic actions of rosuvastatin confer renal benefits in the diabetic Apo-E knockout mouse. *Am J Physiol Renal Physiol* 299: F528–F535, 2010
13. Ohshiro Y, Ma RC, Yasuda Y, Hiraoka-Yamamoto J, Clermont AC, Isshiki K, Yagi K, Arikawa E, Kern TS, King GL: Reduction of diabetes-induced oxidative stress, fibrotic cytokine expression, and renal dysfunction in protein kinase Cbeta-null mice. *Diabetes* 55: 3112–3120, 2006
14. Gray SP, Di Marco E, Okabe J, Szyndralewiez C, Heitz F, Montezano AC, de Haan JB, Koulis C, El-Osta A, Andrews KL, Chin-Dusting JP, Touyz RM, Wingler K, Cooper ME, Schmidt HH, Jandeleit-Dahm KA: NADPH oxidase 1 plays a key role in diabetes mellitus-accelerated atherosclerosis. *Circulation* 127: 1888–1902, 2013
15. Block K, Gorin Y, Abboud HE: Subcellular localization of Nox4 and regulation in diabetes. *Proc Natl Acad Sci U S A* 106: 14385–14390, 2009
16. Geiszt M, Kopp JB, Várnai P, Leto TL: Identification of renox, an NAD(P)H oxidase in kidney. *Proc Natl Acad Sci U S A* 97: 8010–8014, 2000
17. Gorin Y, Block K: Nox4 and diabetic nephropathy: With a friend like this, who needs enemies? *Free Radic Biol Med* 61C: 130–142, 2013
18. Shiose A, Kuroda J, Tsuruya K, Hirai M, Hirakata H, Naito S, Hattori M, Sakaki Y, Sumimoto H: A novel superoxide-producing NAD(P)H oxidase in kidney. *J Biol Chem* 276: 1417–1423, 2001
19. Gorin Y, Block K, Hernandez J, Bhandari B, Wagner B, Barnes JL, Abboud HE: Nox4 NAD(P)H oxidase mediates hypertrophy and fibronectin expression in the diabetic kidney. *J Biol Chem* 280: 39616–39626, 2005
20. Babelova A, Avaniadi D, Jung O, Fork C, Beckmann J, Kosowski J, Weissmann N, Anilkumar N, Shah AM, Schaefer L, Schröder K, Brandes RP: Role of Nox4 in murine models of kidney disease. *Free Radic Biol Med* 53: 842–853, 2012
21. Nlandu Khodo S, Dizin E, Sossauer G, Szanto I, Martin PY, Feraille E, Krause KH, de Seigneux S: NADPH-oxidase 4 protects against kidney fibrosis during chronic renal injury. *J Am Soc Nephrol* 23: 1967–1976, 2012
22. Aoyama T, Paik YH, Watanabe S, Laleu B, Gaggini F, Fioraso-Cartier L, Molango S, Heitz F, Merlot C, Szyndralewiez C, Page P, Brenner DA: Nicotinamide adenine dinucleotide phosphate oxidase in experimental liver fibrosis: GKT137831 as a novel potential therapeutic agent. *Hepatology* 56: 2316–2327, 2012
23. Cooper ME, Vranes D, Youssef S, Stacker SA, Cox AJ, Rizkalla B, Casley DJ, Bach LA, Kelly DJ, Gilbert RE: Increased renal expression of vascular endothelial growth factor (VEGF) and its receptor VEGFR-2 in experimental diabetes. *Diabetes* 48: 2229–2239, 1999
24. Laurindo FR, Fernandes DC, Santos CX: Assessment of superoxide production and NADPH oxidase activity by HPLC analysis of dihydroethidium oxidation products. *Methods Enzymol* 441: 237–260, 2008
25. Chow FY, Nikolic-Paterson DJ, Ozols E, Atkins RC, Rollin BJ, Tesch GH: Monocyte chemoattractant protein-1 promotes the development of diabetic renal injury in streptozotocin-treated mice. *Kidney Int* 69: 73–80, 2006
26. Cooper ME, Mundel P, Boner G: Role of nephrin in renal disease including diabetic nephropathy. *Semin Nephrol* 22: 393–398, 2002
27. Herman-Edelstein M, Thomas MC, Thallas-Bonke V, Saleem M, Cooper ME, Kantharidis P: Dedifferentiation of immortalized human podocytes in response to transforming growth factor-β: A model for diabetic podocytopathy. *Diabetes* 60: 1779–1788, 2011
28. Chai Z, Dai A, Tu Y, Li J, Wu T, Wang Y, Hale LJ, Koentgen F, Thomas MC, Cooper ME: Genetic deletion of CDA1 retards diabetes associated renal injury. *J Am Soc Nephrol* 24: 1782–1792, 2013
29. Lassila M, Seah KK, Allen TJ, Thallas V, Thomas MC, Candido R, Burns WC, Forbes JM, Calkin AC, Cooper ME, Jandeleit-Dahm KA: Accelerated nephropathy in diabetic apolipoprotein e-knockout mouse: Role of advanced glycation end products. *J Am Soc Nephrol* 15: 2125–2138, 2004
30. Altenhöfer S, Kleikers PW, Radermacher KA, Scheurer P, Rob Hermans JJ, Schiffers P, Ho H, Wingler K, Schmidt HH: The NOX toolbox: Validating the role of NADPH oxidases in physiology and disease. *Cell Mol Life Sci* 69: 2327–2343, 2012
31. Wind S, Beuerlein K, Eucker T, Müller H, Scheurer P, Armitage ME, Ho H, Schmidt HH, Wingler K: Comparative pharmacology of chemically distinct NADPH oxidase inhibitors. *Br J Pharmacol* 161: 885–898, 2010

32. Fujii M, Inoguchi T, Maeda Y, Sasaki S, Sawada F, Saito R, Kobayashi K, Sumimoto H, Takayanagi R: Pitavastatin ameliorates albuminuria and renal mesangial expansion by downregulating NOX4 in db/db mice. *Kidney Int* 72: 473–480, 2007
33. Ford BM, Eid AA, Göőz M, Barnes JL, Gorin YC, Abboud HE: ADAM17 mediates Nox4 expression and NADPH oxidase activity in the kidney cortex of OVE26 mice. *Am J Physiol Renal Physiol* 305: F323–F332, 2013
34. Brosius FC: Susceptible mice: Identifying a diabetic nephropathy disease locus using a murine model. *Kidney Int* 78: 431–432, 2010
35. Bondi CD, Manickam N, Lee DY, Block K, Gorin Y, Abboud HE, Barnes JL: NAD(P)H oxidase mediates TGF-beta1-induced activation of kidney myofibroblasts. *J Am Soc Nephrol* 21: 93–102, 2010
36. Sedeek M, Callera G, Montezano A, Gutsol A, Heitz F, Szyndralewiez C, Page P, Kennedy CR, Burns KD, Touyz RM, Hébert RL: Critical role of Nox4-based NADPH oxidase in glucose-induced oxidative stress in the kidney: Implications in type 2 diabetic nephropathy. *Am J Physiol Renal Physiol* 299: F1348–F1358, 2010
37. Piwkowska A, Rogacka D, Audzeyenka I, Jankowski M, Angielski S: High glucose concentration affects the oxidant-antioxidant balance in cultured mouse podocytes. *J Cell Biochem* 112: 1661–1672, 2011
38. Flyvbjerg A, Dagnaes-Hansen F, De Vriese AS, Schrijvers BF, Tilton RG, Rasch R: Amelioration of long-term renal changes in obese type 2 diabetic mice by a neutralizing vascular endothelial growth factor antibody. *Diabetes* 51: 3090–3094, 2002
39. Li J, Wang JJ, Yu Q, Chen K, Mahadev K, Zhang SX: Inhibition of reactive oxygen species by Lovastatin downregulates vascular endothelial growth factor expression and ameliorates blood-retinal barrier breakdown in db/db mice: Role of NADPH oxidase 4. *Diabetes* 59: 1528–1538, 2010
40. Kleinschnitz C, Grund H, Wingler K, Armitage ME, Jones E, Mittal M, Barit D, Schwarz T, Geis C, Kraft P, Barthel K, Schuhmann MK, Herrmann AM, Meuth SG, Stoll G, Meurer S, Schrewe A, Becker L, Gailus-Durner V, Fuchs H, Klopstock T, de Angelis MH, Jandeleit-Dahm K, Shah AM, Weissmann N, Schmidt HH: Post-stroke inhibition of induced NADPH oxidase type 4 prevents oxidative stress and neurodegeneration. *PLoS Biol* 8: 8, 2010
41. Park HS, Chun JN, Jung HY, Choi C, Bae YS: Role of NADPH oxidase 4 in lipopolysaccharide-induced proinflammatory responses by human aortic endothelial cells. *Cardiovasc Res* 72: 447–455, 2006
42. Kiritoshi S, Nishikawa T, Sonoda K, Kukidome D, Senokuchi T, Matsuo T, Matsumura T, Tokunaga H, Brownlee M, Araki E: Reactive oxygen species from mitochondria induce cyclooxygenase-2 gene expression in human mesangial cells: Potential role in diabetic nephropathy. *Diabetes* 52: 2570–2577, 2003
43. Nishikawa T, Edelstein D, Du XL, Yamagishi S, Matsumura T, Kaneda Y, Yorek MA, Beebe D, Oates PJ, Hammes HP, Giardino I, Brownlee M: Normalizing mitochondrial superoxide production blocks three pathways of hyperglycaemic damage. *Nature* 404: 787–790, 2000
44. Chabrashvili T, Kitiyakara C, Blau J, Karber A, Aslam S, Welch WJ, Wilcox CS: Effects of ANG II type 1 and 2 receptors on oxidative stress, renal NADPH oxidase, and SOD expression. *Am J Physiol Regul Integr Comp Physiol* 285: R117–R124, 2003
45. Nishiyama A, Yoshizumi M, Hitomi H, Kagami S, Kondo S, Miyatake A, Fukunaga M, Tamaki T, Kiyomoto H, Kohno M, Shokoji T, Kimura S, Abe Y: The SOD mimetic tempol ameliorates glomerular injury and reduces mitogen-activated protein kinase activity in Dahl salt-sensitive rats. *J Am Soc Nephrol* 15: 306–315, 2004
46. Gurley SB, Coffman TM: The renin-angiotensin system and diabetic nephropathy. *Semin Nephrol* 27: 144–152, 2007
47. Kobori H, Kamiyama M, Harrison-Bernard LM, Navar LG: Cardinal role of the intrarenal renin-angiotensin system in the pathogenesis of diabetic nephropathy. *J Investig Med* 61**:** 256–264, 2013
48. Valente AJ, Yoshida T, Murthy SN, Sakamuri SS, Katsuyama M, Clark RA, Delafontaine P, Chandrasekar B: Angiotensin II enhances AT1-Nox1 binding and stimulates arterial smooth muscle cell migration and proliferation through AT1, Nox1, and interleukin-18. *Am J Physiol Heart Circ Physiol* 303: H282–H296, 2012
49. Itani HA, Dikalov S, Harrison DG: Knock, knock: Who's there?: Nox1. *Circulation* 127: 1850–1852, 2013
50. You YH, Okada S, Ly S, Jandeleit-Dahm K, Barit D, Namikoshi T, Sharma K: Role of Nox2 in diabetic kidney disease. *Am J Physiol Renal Physiol* 304: F840–F848, 2013
51. Sedeek M, Montezano AC, Hebert RL, Gray SP, Di Marco E, Jha JC, Cooper ME, Jandeleit-Dahm K, Schiffrin EL, Wilkinson-Berka JL, Touyz RM: Oxidative stress, Nox isoforms and complications of diabetes—potential targets for novel therapies. *J Cardiovasc Transl Res* 5: 509–518, 2012
52. Jiang JX, Chen X, Serizawa N, Szyndralewiez C, Page P, Schröder K, Brandes RP, Devaraj S, Török NJ: Liver fibrosis and hepatocyte apoptosis are attenuated by GKT137831, a novel NOX4/NOX1 inhibitor in vivo. *Free Radic Biol Med* 53: 289–296, 2012
53. Gavazzi G, Banfi B, Deffert C, Fiette L, Schappi M, Herrmann F, Krause KH: Decreased blood pressure in NOX1-deficient mice. *FEBS Lett* 580: 497–504, 2006
54. Sheehan AL, Carrell S, Johnson B, Stanic B, Banfi B, Miller FJ Jr: Role for Nox1 NADPH oxidase in atherosclerosis. *Atherosclerosis* 216: 321–326, 2011
55. Laleu B, Gaggini F, Orchard M, Fioraso-Cartier L, Cagnon L, Houngninou-Molango S, Gradia A, Duboux G, Merlot C, Heitz F, Szyndralewiez C, Page P: First in class, potent, and orally bioavailable NADPH oxidase isoform 4 (Nox4) inhibitors for the treatment of idiopathic pulmonary fibrosis. *J Med Chem* 53: 7715–7730, 2010
56. Watson AM, Li J, Schumacher C, de Gasparo M, Feng B, Thomas MC, Allen TJ, Cooper ME, Jandeleit-Dahm KA: The endothelin receptor antagonist avosentan ameliorates nephropathy and atherosclerosis in diabetic apolipoprotein E knockout mice. *Diabetologia* 53: 192–203, 2010
57. Krege JH, Hodgin JB, Hagaman JR, Smithies O: A noninvasive computerized tail-cuff system for measuring blood pressure in mice. *Hypertension* 25: 1111–1115, 1995
58. Watson AM, Gray SP, Jiaze L, Soro-Paavonen A, Wong B, Cooper ME, Bierhaus A, Pickering R, Tikellis C, Tsorotes D, Thomas MC, Jandeleit-Dahm KA: Alagebrium reduces glomerular fibrogenesis and inflammation beyond preventing RAGE activation in diabetic apolipoprotein E knockout mice. *Diabetes* 61: 2105–2113, 2012
59. Calkin AC, Giunti S, Jandeleit-Dahm KA, Allen TJ, Cooper ME, Thomas MC: PPAR-alpha and -gamma agonists attenuate diabetic kidney disease in the apolipoprotein E knockout mouse. *Nephrol Dial Transplant* 21**:** 2399–2405, 2006
60. Saleem MA, O'Hare MJ, Reiser J, Coward RJ, Inward CD, Farren T, Xing CY, Ni L, Mathieson PW, Mundel P: A conditionally immortalized human podocyte cell line demonstrating nephrin and podocin expression. *J Am Soc Nephrol* 13: 630–638, 2002
61. Okabe J, Orlowski C, Balcerczyk A, Tikellis C, Thomas MC, Cooper ME, El-Osta A: Distinguishing hyperglycemic changes by Set7 in vascular endothelial cells. *Circ Res* 110: 1067–1076, 2012

This article contains supplemental material online at http://jasn.asnjournals.org/lookup/suppl/doi:10.1681/ASN.2013070810/-/DCSupplemental.

Supplementary Data

Genetic targeting or pharmacologic inhibition of NADPH oxidase Nox4 provide renoprotection in long-term diabetic nephropathy

Jay C Jha[1,7], Stephen P Gray[1], David Barit[1], Jun Okabe[2] , Assam El-Osta[2], Tamehachi Namikoshi[1,3], Vicki Thallas[1], Kirstin Wingler[4], Cedric Szyndralewiez[5], Freddy Heitz[5], Rhian M Touyz[6], Mark E Cooper[1,7], Harald HHW Schmidt[4,*] and Karin A Jandeleit-Dahm[1,7*]

[1] JDRF Danielle Alberti Memorial Centre for Diabetic Complications, Diabetic Complications Division, [2]Human Epigenetics Laboratory, Baker IDI Heart & Diabetes Institute, Melbourne

[3]Department of Nephrology and Hypertension, Kawasaki Medical School, Kurashiki, Japan [4]Department of Pharmacology, Cardiovascular Research Institute Maastricht (CARIM), Faculty of Medicine, Health & Life Science, Maastricht University, Netherlands

[5]Genkyotex SA, Geneva, Switzerland

[6]Ottawa Hospital Research Institute, Ottawa, Canada and Institute of Cardiovascular and Medical Sciences, University of Glasgow, UK

[7]Department of Medicine, Monash University, Australia

SUPPLEMENTARY FIGURES LEGENDS AND TABLES

Supplemental Figure 1.

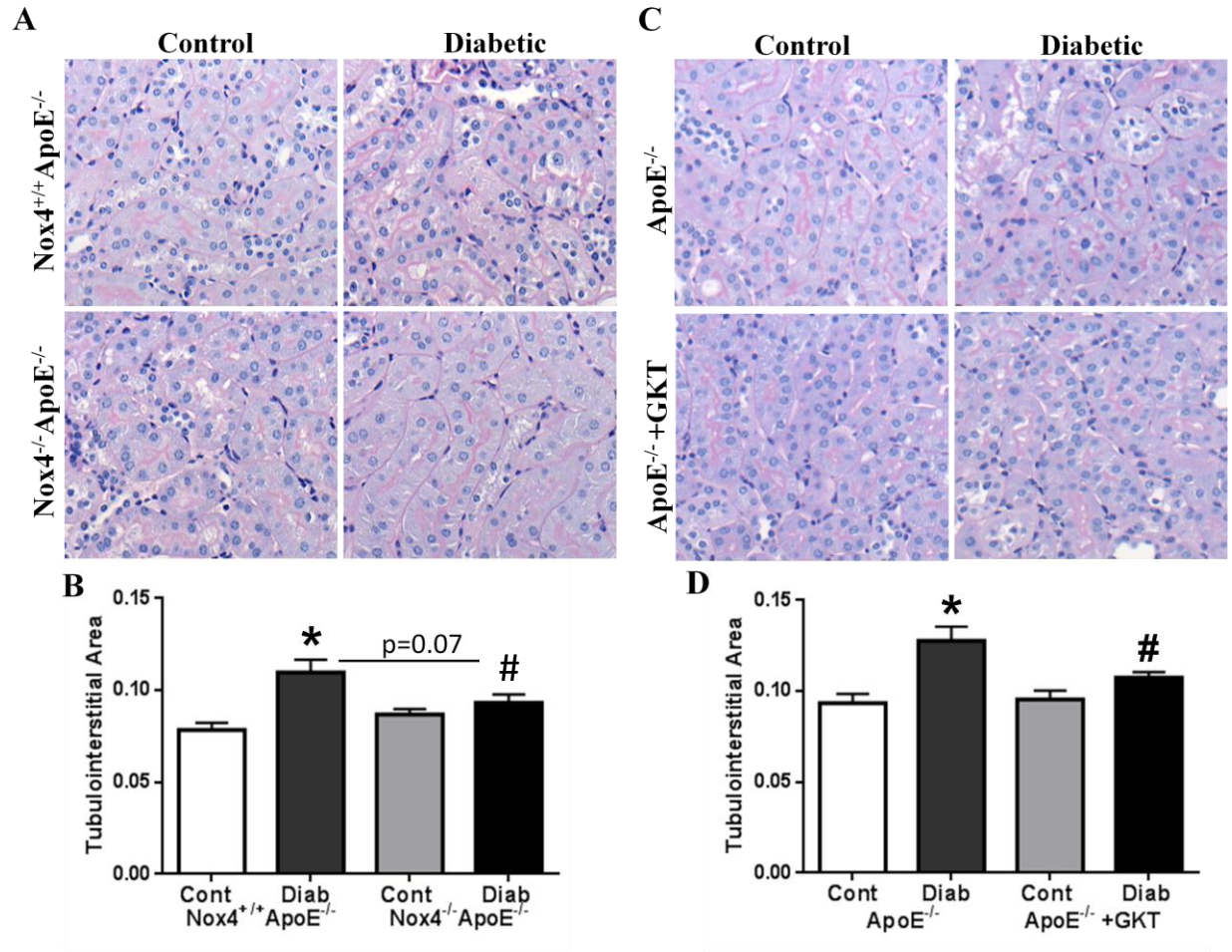

Supplemental Figure1. Analysis of tubulointerstitial area by point counting method in the tubulues of renal cortex after 20 weeks of study in respective control and diabetic *Nox4*$^{+/+}$*ApoE*$^{-/-}$ and *Nox4*$^{-/-}$*ApoE*$^{-/-}$ mice (A and B) and in respective control and diabetic *ApoE*$^{-/-}$ and ApoE$^{-/-}$ *+GKT* mice (C and D). Data are the mean ± SEM. *p<0.05 versus control *Nox4*$^{+/+}$*ApoE*$^{-/-}$ and control *ApoE*$^{-/-}$ *mice*; $^{\#}$p<0.05 versus diabetic *ApoE*$^{-/-}$ mice, $^{\#}$p=0.07 versus diabetic *Nox4*$^{+/+}$*ApoE*$^{-/-}$ mice. Cont, control; Diab, diabetes.

Supplemental Figure 2.

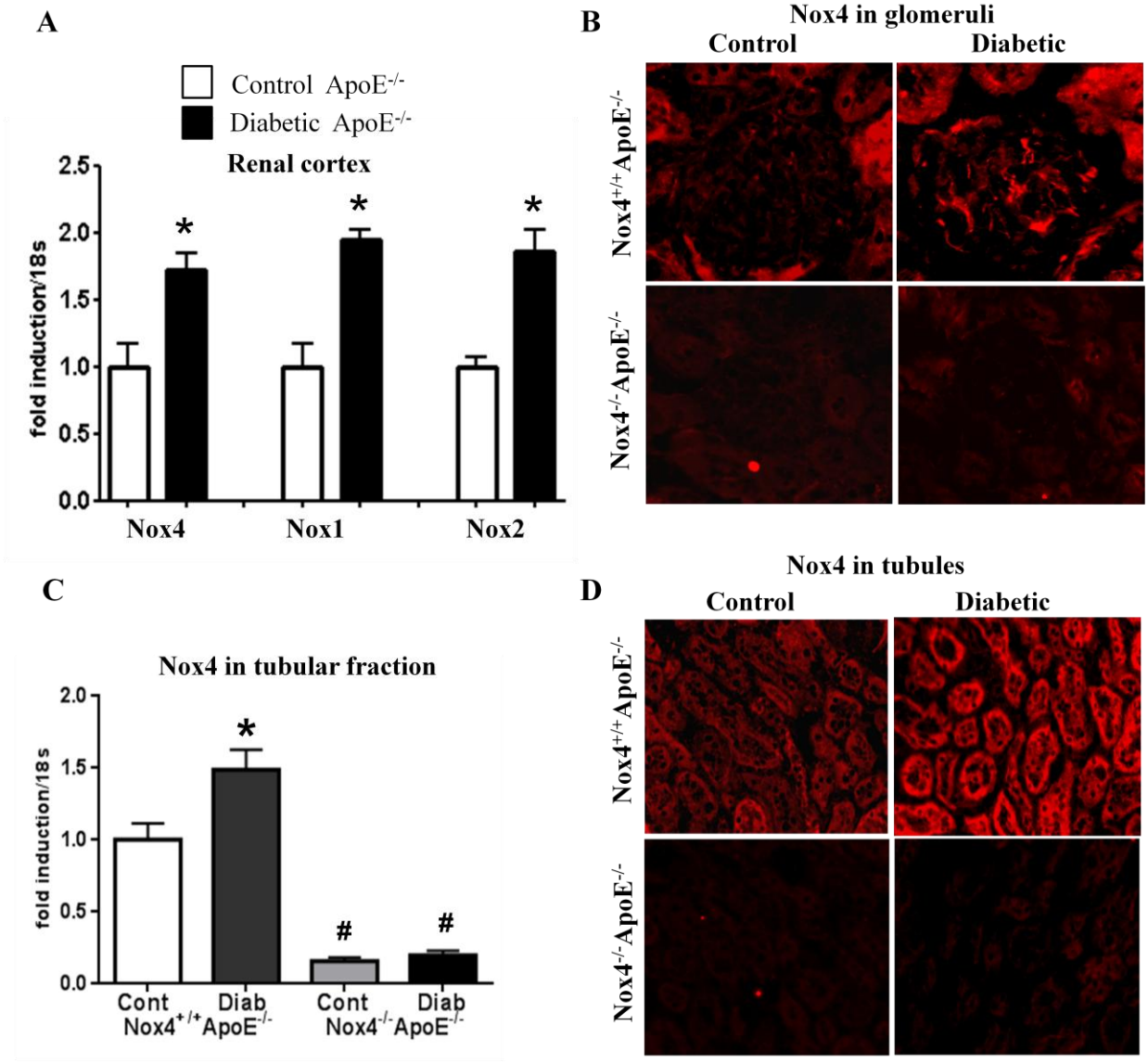

Supplemental Figure 2. Analysis of Nox1, Nox2 and Nox4 mRNA levels in the renal cortex of control and diabetic *ApoE*$^{-/-}$ mice (A) and Nox4 mRNA expression in tubular fraction of renal cortex (C). Analysis of protein expression of Nox4 in renal cortex and tubules after 20 weeks of study in respective control and diabetic *Nox4*$^{+/+}$*ApoE*$^{-/-}$ and *Nox4*$^{-/-}$*ApoE*$^{-/-}$ mice by immunofluorescence (B and D). Data are the mean ± SEM. $^{*}p<0.05$ versus respective control *ApoE*$^{-/-}$ or *Nox4*$^{+/+}$*ApoE*$^{-/-}$ mice; #p<0.05 versus control or diabetic *Nox4*$^{+/+}$*ApoE*$^{-/-}$ mice. Cont, control; Diab, diabetes.

Supplemental Figure 3.

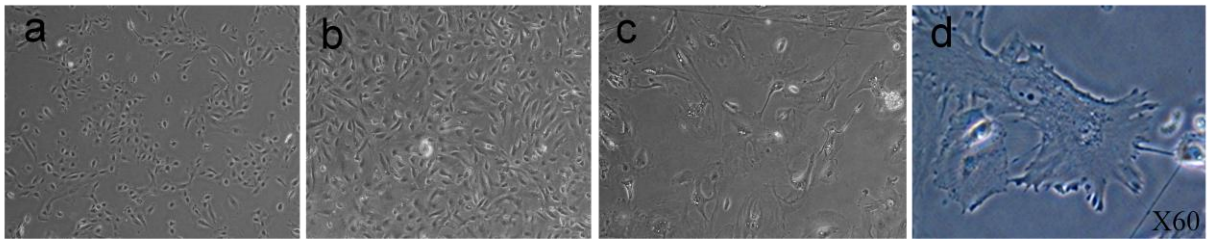

Supplemental Figure 3. (a) Podocytes grown under permissive conditions (at 33°C display more characteristic cobblestone morphology. The cells form an epithelial monolayer as they reach confluence. (b) Differentiating (2 day) and (c and d) differentiated podocytes grown under nonpermissive conditions (10-14 days at 37°C). Under nonpermissive conditions, the cells develop interdigitating processes, which are only connected at sites of process interdigitations. On day 10-14, large, flat arborized cells with well-developed prominent processes can be seen.

Supplemental Figure 4.

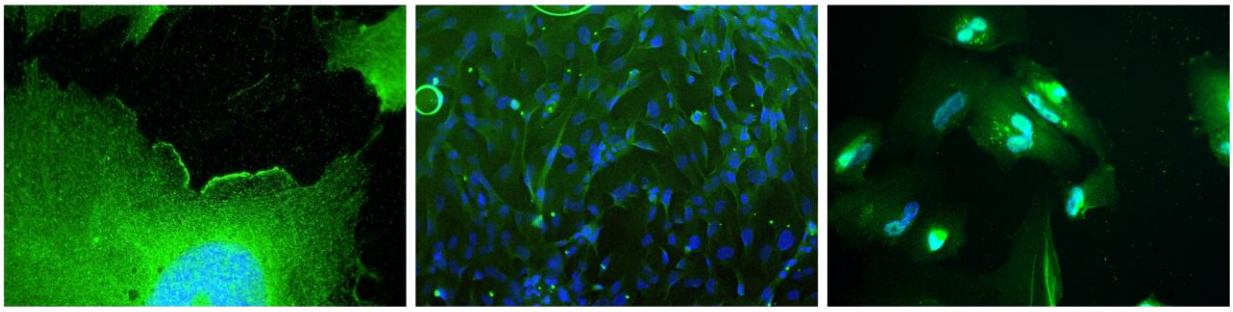

Supplemental Figure 4. Immunofluorescence staining for nephrin, synaptopodin and WT-1, with a blue nuclear counterstain (DAPI). Under nonpermissive conditions (at 37°C), the podocytes undergo growth arrest, display the typical arborized pattern of foot process extensions, and express markers of mature podocytic differentiation in vitro.

Supplemental Figure 5.

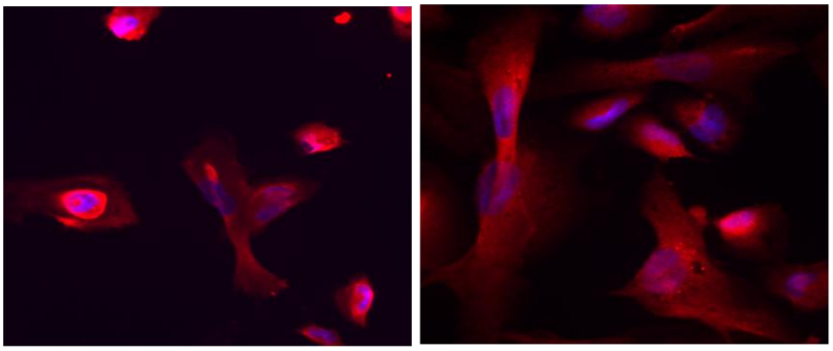

Supplemental Figure 5. Analysis of protein expression of Nox4 in podocytes cultured in NG (5mM) and HG (25mM) medium by immunofluorescence. NG, normal glucose; HG, high glucose.

Supplemental Figure 6.

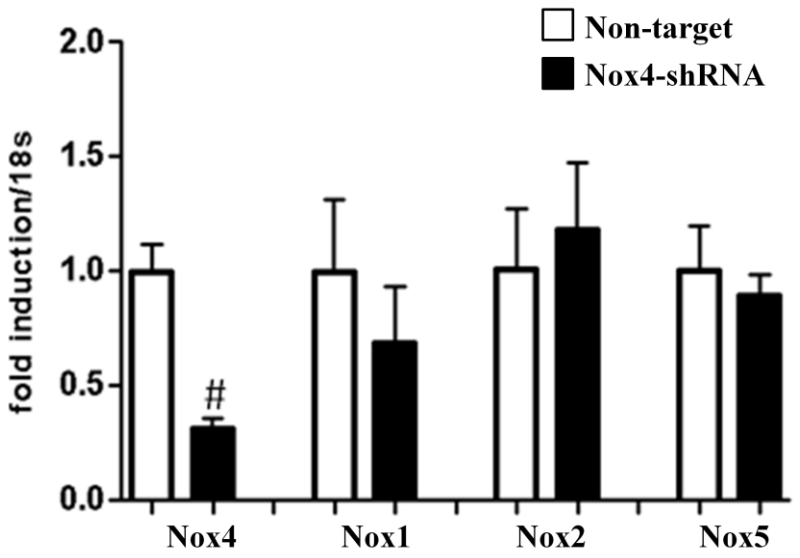

Supplemental Figure 6. shRNA to Nox4 downregulates Nox4 but not the Nox1, Nox2 or Nox5 mRNA levels in human podocytes. Analysis of Nox isoform mRNA levels in cultured differentiated human podocytes in normal glucose RPMI medium. Data are the mean ± SEM. $^{\#}p<0.01$ vs. Non-target.

Supplemental Table 1. Mouse probe and primer sequences for qRT-PCR

Genes	Probe Sequence 5'FAM-3"TAMRA	Forward Primer 5'-3'	Reverse Primer 5'-3'
Nox1	CTAGAATAGCTACTGCCCACC	GACCAATGTGGGACAATGAGTTT	CCCCCACCGCAGACTTG
Nox2	CAACTGGACAGGAACCT	AGTGCGTGTTGCTCGACAAG	CCAAGCTACCATCTTATGGAAAGT
Nox4	CATTTTGCTATTTCATCAAA	AAAAATATCACACACTGAATTCGAGACT	TGGGTCCACAGCAGAAAACTC
MCP1	AATGGGTCCAGACATAC	GTCTGTGCTGACCCCAAGAAG	TGGTTCCGATCCAGGTTTTTA
NFκB-p65	AGCTCAAGATCTGCCG	TCTCACATCCGATTTTTGATAACC	CGAGGCAGCTCCCAGAGTT

FAM, 5'-Fluorescein; MCP, monocyte chemoattractant protein 1; NFκβ-p65, nuclear factor kappa-light-chain-enhancer of activated B cells-p65.

Supplemental Table 2. Human probe and primer sequences for qRT-PCR

Genes	Probe Sequence 5'FAM-3"TAMRA	Forward Primer 5'-3'	Reverse Primer 5'-3'
Nox1	AAAGCAATTGGATCACAAC	TTGCAGCCGCACACTGA	GGCCACCAGCTTGTGGAA
Nox2	CCTCCTGCCATGACT	AGAGGGTTGGAGGTGGAGAATT	GCACAAGGAGCAGGACTAGATGA
Nox4	TCCATTTGCATCAATACT	GGCTGGAGGCATTGGAGTAA	CCAGTCATCCAACAGGGTGTT
P47phox	TGAGCCATACGTCGCC	CCCTGAGCCCAACTATGCA	CCACAGCAGTGTAGGCCTTGA
Collagen IV	ATTTGCGTAACTAACACACC	CAATATGAAAACCGTAAAGTGCCTTATA	CAGCAAGTAGAGGTCAATGAAGCA
Fibronectin	TGCCATTTGCTCCTGC	AGAACAGTGGCAGAAGGAATATCTC	CCCGCTGGCCTCCAA
CTGF	ACTGCCTGGTCCAGAC	GCGGCTTACCGACTGGAA	GGAACAGGCGCTCCACTCT
α-SMA	TGCCAGATCTTTTCC	ACCCTGAAGTACCCGATAGAACAT	CAACACGAAGCTCATTGTAGAAAGA
VEGF	CCCACTGAGGAGTCC	CGAGGGCCTGGAGTGTGT	CGCATAATCTGCATGGTGATG
MCP1	CAGGAAACCAATATCCA	CAAAGCAGGGCTCGAGTTG	CCTGGGACTAGACTTGATGTCTCA
NFκB-p65	AGCTCAAGATCTGCCG	CTCATCCCATCTTTGACAATCGT	TGCACCTTGTCACACAGTAGGAA

FAM, 5'-Fluorescein; α-SMA, smooth muscle actin; CTGF, connective tissue transforming growth factor; VEGF, vascular endothelial growth factor ; MCP1, monocyte chemoattractant protein 1; NFκβ-p65, nuclear factor kappa-light-chain-enhancer of activated B cells-p65.

CONCISE METHODS

Immunofluorescence

Human podocytes were grown on coverslips, washed twice with PBS. Renal frozen sections (4μm) and podocytes were fixed in 4% paraformaldehyde for 15 minutes, permeabilized using 0.1% tritonX and incubated in a blocking buffer (1% BSA, 0.25% TritonX in PBS, pH 7.4). Primary and secondary antibodies were diluted in blocking buffer, and the tissue sections and cells with primary antibodies were incubated overnight at 4°C. Coverslips were then mounted onto glass microscope slides and tissue sections were coversliped using Prolog Gold antifade reagent with DAPI (Invitrogen, Carlsbad, CA) or TO-PRO-3 (Invitrogen). Primary antibodies used included the following: Nox4 (rabbit polyclonal anti-Nox4, Abcam, Cambridge, MA, USA), nephrin (Santa Cruz Biotechnology, Santa Cruz, CA), synaptopodin (Santa Cruz Biotechnology, Santa Cruz, CA) and WT-1 (Santa Cruz Biotechnology, Santa Cruz, CA). Secondary antibodies used for immunofluorescence detection included Alexa Fluor 488 (rabbit anti-goat, Invitrogen, Eugene, Oregon, USA), Alexa Fluor 546 (goat anti-rabbit, Invitrogen, Eugene, Oregon, USA). All stained sections and cells were examined using an Olympus (Tokyo, Japan) BX61 fluorescence microscope, and images were captured on a Zeiss 510 Meta laser scanning confocal microscope (Zeiss, Germany) using LSM 510 software (version 3.2 SP2; Zeiss) or an Olympus BX61 fluorescence microscope.

Tubulointerstitial (TI) Area

Three micrometer kidney sections were stained with periodic acid–Schiff (PAS) for assessment of tubulointerstitial (TI) area in the renal cortex by using a point-counting technique routinely used method [1]. Briefly, in each field, 100 points were counted on a 1 cm^2 eyepiece graticule with 10 equidistant grid lines. A total of 12 high-power fields (x400) per section were counted for each animal in all groups in the corticomedullary field. Each high-power field was 0.076mm^2, and the total area counted on the power slide was 0.91mm^2. Tubulointerstitial area = number of tubulointerstitial grid intersections/total number of intersections.

RT-PCR in tubular fraction of renal cortex

Tubules were isolated from the renal cortex by sieving method. Briefly, medulla was separated from the frozen kidney. Tubular fraction was obtained by mincing with the renal cortex with scalpel, and grinding the homogenate through a 100-mm disposable filter using a rubber syringe plunger. The saline-washed flow through material was passed through a 70-mm disposable filter, collected, and stored as the tubular fraction which was used for the RNA extraction for gene expression analysis by RT-PCR.

References

1. Hewitson TD, Darby IA, Bisucci T et al. Evolution of tubulointerstitial fibrosis in experimental renal infection and scarring. J Am Soc Nephrol 1998; 9: 632–642.